evidence, especially from transgenic and knockout mouse models (4, 8). In these models, mature hepatic SREBP-1c protein levels determine mRNA expression levels for a battery of lipogenic genes in the liver. Moreover, mature hepatic SREBP-1c is physiologically regulated by nutrient availability (i.e., it is downregulated when animals are starved and upregulated when they are refed), thereby adjusting lipogenic gene expression levels to the nutritional conditions (9). Thus, regarding its role in the liver, SREBP-1c is now well established as a key transcription factor for the regulation of lipogenic gene expression and by extension triglyceride storage in liver (10, 11).

Despite the extensive knowledge gained in recent years regarding the role of SREBP-1 in lipogenesis in liver, its physiological role in adipocytes remains obscure. Although the mRNA expression of SREBP-1c in adipocytes is also drastically altered by dietary conditions, we have reported that targeted disruption of the SREBP-1 gene scarcely affected the dynamic changes of lipogenic gene expression in adipose tissue (4). Conversely, the impact of SREBP-1c overexpression in adipocytes was also evaluated in transgenic mice; however, it disrupted the differentiation processes of adipocytes, resulting in lipodystrophy. Hence, the effect of SREBP-1c on lipogenic gene regulation in adipocytes was not able to be evaluated (12), although ectopic overexpression of SREBP-1a drives fatty acid synthesis in the adipose tissue of transgenic mice (13).

These situations prompted us to investigate the effects of SREBP-1c activation in adipocytes by stimulating the SREBP-1c promoter. We and others have found that liver X receptors (LXRs), nuclear receptor-type transcription factors, activate the transcription of the SREBP-1c gene through binding to LXR elements in the promoter, together with retinoid X receptors (RXRs) (14, 15).

Here, we show that the stimulation of the SREBP-1c gene with LXR agonist has negligible effects on the expression of lipogenic enzymes in adipocytes, despite a concomitant increase in nuclear active SREBP-1c, indicating that the transcriptional activity of SREBP-1c against lipogenic genes is almost nil in adipocytes in contrast to hepatocytes. In fact, luciferase reporter gene assays demonstrated that the recombinant nuclear active form of SREBP-1c had far lower activity for the FAS promoter in 3T3-L1 adipocytes than in HepG2 hepatoma cells. Consistent with these observations, chromatin immunoprecipitation (ChIP) assays revealed that SREBP-1 is not recruited to the functional *cis* element on the FAS promoter in LXR-activated adipocytes. Therefore, lipogenic genes are controlled almost independently of SREBP-1c in adipocytes, and the triglyceride biosynthetic pathway is differently regulated between liver and adipose tissue.

MATERIALS AND METHODS

Materials

The synthetic LXR agonist T0901317 was purchased from Cayman Chemical (Ann Arbor, MI). The RXR agonist LG100268 was synthesized as described elsewhere (16). Standard laboratory chow (MF; composed of 60% carbohydrate, 13% fat, and 27% protein on a caloric basis) was obtained from Oriental Yeast (Tokyo, Japan). Other materials were purchased from Sigma unless indicated otherwise.

Animals

Eight week old male Wister rats and 8 week old male C57BL/6J mice were purchased from CLEA (Tokyo, Japan). All animals were maintained in a temperature-controlled environment with a 12 h light/dark cycle and were given free access to standard chow and water. The dosage of T0901317 (suspended with 0.9% carboxymethylcellulose, 9.95% polyethylene glycol 400, and 0.05% Tween 80, administered orally) was 10 mg/kg for rats and 50 mg/kg for mice. Animals were euthanized at 12 h after administration. The protocol of dietary manipulation was as follows: for the fasting group, mice were starved for 24 h and rats were starved for 48 h; for the refeeding group, they were refed at 12 h or 24 h after a 24 h (for mice) or 48 h (for rats) starvation, respectively, unless stated otherwise. All groups of animals in one experiment were euthanized at the same time. SREBP-1-null mice (16 weeks of age, female) on the C57BL/6J background have been reported previously (4).

RNA isolation and Northern blotting

Total RNA from liver, epididymal fat pads, and cultured cells was isolated with Trizol Reagent (Invitrogen), and a 10 μg RNA sample equally pooled among each group was run on a 1% agarose gel containing formaldehyde and transferred to a nylon membrane. cDNA probes were cloned as described previously (4, 17). The probes were labeled with [α-^{32}P]dCTP using the Megaprime DNA Labeling System (Amersham Biosciences). The membranes were hybridized with the radiolabeled probe in Rapid-hyb buffer (Amersham Biosciences) at 65°C and washed in 0.1× SSC buffer with 0.1% SDS at 65°C. Blots were exposed to both Kodak XAR-5 film and the imaging plate for the BAS2000 BIO Imaging Analyzer (Fuji Photo Film, Tokyo, Japan). The quantification results obtained from the BAS2000 system were normalized to the signal generated from 36B4 (acidic ribosomal phosphoprotein P0) mRNA.

Quantitative real-time PCR analysis

Two micrograms of total RNA was reverse-transcribed using the ThermoScript RT-PCR system (Invitrogen). Quantitative real-time PCR was performed using SYBR Green dye (Applied Biosystems, Foster City, CA) in an ABI Prism 7900 PCR instrument (Applied Biosystems). The relative abundance of each transcript was calculated by a standard curve of cycle thresholds for serial dilutions of a cDNA sample and normalized to 36B4. Primer sequences are available upon request.

Nuclear protein extraction from liver and fat

Nuclear extract protein from mouse or rat liver was prepared as described previously (18). Briefly, excised livers (0.5 g) were homogenized in a Polytron in 5 ml of buffer A, which consisted of 10 mM HEPES at pH 7.9, 25 mM KCl, 1 mM EDTA, 2 M sucrose, 10% glycerol, 0.15 mM spermine, and 2 mM spermidine, supplemented with protease inhibitors [6 μg/ml *N*-acetyl-leucyl-leucyl-norleucinal (ALLN; Calbiochem), 2.5 μg/ml pepstatin A, 2 μg/ml leupeptin, 0.1 mM phenylmethylsulfonyl fluoride, and 2.5 μg/ml aprotinin]. Pooled homogenate was then subjected to one stroke of a Teflon pestle in a Potter-Elvejiem homogenizer, followed by filtration through two layers of cheesecloth, and layered over 10 ml of buffer A. After centrifugation at 24,000 rpm on a Beckman SW28 rotor for 1 h at 4°C, the resulting nuclear pellet

was resuspended in a buffer containing 10 mM HEPES at pH 7.9, 100 mM KCl, 2 mM $MgCl_2$, 1 mM EDTA, 1 mM dithiothreitol, and 10% glycerol, supplemented with protease inhibitors, after which 0.1 volume of 5 M NaCl was added. Each mixture was agitated gently for 30 min at 4°C and then centrifuged at 89,000 rpm on a Himac S120AT2 rotor (Hitachi, Tokyo, Japan) for 30 min at 4°C. The supernatant was used as nuclear extract.

Nuclear protein from white adipose tissue was prepared as described previously (19). In brief, fresh epididymal fat pads (~3 g) were rinsed in ice-cold PBS, minced, and homogenized with 10 strokes of a Teflon homogenizer in 15 ml of NDS buffer at 4°C (10 mM Tris-HCl at pH 7.5, 10 mM NaCl, 60 mM KCl, 0.15 mM spermine, 0.5 mM spermidine, 14 mM mercaptoethanol, 0.5 mM EGTA, 2 mM EDTA, 0.5% Nonidet P-40, and 1 mM dithiothreitol) supplemented with protease inhibitors (6 μg/ml ALLN, 2 μg/ml leupeptin, 2.5 μg/ml aprotinin, 2.5 μg/ml pepstatin A, and 0.1 mM phenylmethylsulfonyl fluoride). The Nonidet P-40 concentration was increased to 1%, and nuclei were pelleted at 700 *g* for 10 min, washed once with 25 ml of NDS buffer (1% Nonidet P-40), filtered through 70 μm mesh, pelleted at 500 *g* for 10 min, resuspended in 1 volume of 1% citric acid, lysed by the addition of 2.5 volumes of 0.1 M Tris-HCl, 2.5% SDS, and 0.1 M dithiothreitol, sonicated briefly, and heated to 90°C for 5 min. Aliquots of nuclear protein (20 μg) were subjected to SDS-PAGE.

Primary culture of rat preadipocytes

Fibroblastic preadipocytes were isolated from epididymal fat pads of Wister rats by collagenase digestion as described previously (20). In brief, the epididymal fat pads from male Wister rat were removed and minced in KRBH buffer (130 mM NaCl, 5.2 mM KCl, 1.3 mM KH_2PO_4, 2.7 mM $CaCl_2$, 1.3 mM $MgSO_4$, 24.8 mM $NaHCO_3$, and 10 mM HEPES at pH 7.4) supplemented with 3% (w/v) BSA, 2 mM glucose, and 200 nM adenosine. After digestion by collagenase (type II; 1.5 mg/ml) at 37°C for 1 h in a shaking water bath, the digest was filtered through sterile 250 μm nylon mesh. The adipocytes were allowed to float to the top of the tube and the infranatant was collected, passed through a 25 μm stainless steel filter, and centrifuged at 250 *g* for 10 min. The pellet was resuspended in MEM-α medium (Invitrogen) with 10% FBS supplemented with penicillin and streptomycin (100 U/ml and 100 μg/ml, respectively; Invitrogen). Red blood cells were lysed by hypotonic shock (21). The cells were plated on 60 mm culture dishes at a density of 6×10^5 cells/well. Medium was changed every 2 days. After the cells reached confluence, differentiation was induced in MEM-α medium with 10% FBS by the addition of 0.5 mM isobutylmethylxanthine (Wako), 0.25 μM dexamethasone, 5 μg/ml bovine insulin, and 1 μM pioglitazone (provided by Takeda Pharmaceutical). The differentiation of cells was morphologically confirmed. Differentiated adipocytes were treated with either vehicle (ethanol) or 10 μM T0901317 for 12 h in MEM-α medium containing the indicated amounts of glucose and insulin.

Primary culture of rat hepatocytes

Hepatocytes were isolated from nonfasted 4 week old Wister rats by the collagenase perfusion method as described previously (22). Cells were resuspended in DMEM containing 25 mM glucose supplemented with 5% FBS and seeded on collagen-coated 100 mm dishes at a final density of 4×10^4 cells/cm^2. After 4 h, attached cells were cultured with Medium 199 containing Earle's salts (Invitrogen) and 5% FBS. After incubation for 20 h, cells were treated with either vehicle (ethanol) or 10 μM T0901317 for 12 h in similar medium containing the indicated amounts of glucose and insulin.

Preparation of nuclear extracts from cultured cells

Nuclear proteins from cultured cells were extracted as described previously (23). In brief, 2 h before collection, ALLN (6 μg/ml) was added to the medium. After collection, cells were resuspended in buffer A (10 mM HEPES at pH 7.6, 1 mM KCl, 1.5 mM $MgCl_2$, 1 mM EDTA, and 1 mM EGTA) and passed through a 26 gauge needle 20 times and then briefly centrifuged. The pellet, containing the nuclei, was resuspended in buffer B (20 mM HEPES at pH 7.6, 25% glycerol, 0.42 M NaCl, 1.5 mM $MgCl_2$, 1 mM EDTA, 1 mM EGTA, and 0.5 mM dithiothreitol) and rotated at 4°C for 15 min and then centrifuged at 15,000 *g* for 20 min. The supernatant was collected as nuclear extract. Whole cell lysates were harvested with a buffer (20 mM Tris-HCl at pH 7.4) containing detergents (1% Triton X-100, 0.1% SDS, and 1% sodium deoxycholate) and protease inhibitors according to a standard protocol.

Immunoblotting of SREBP proteins

Membrane fractions from livers and epididymal fat pads were prepared as described previously (18). Aliquots of nuclear extract (20 μg) and membrane fraction (50 μg) proteins were subjected to SDS-PAGE. Immunoblot analysis was performed using the ECL Western Blotting Detection System (Amersham Biosciences) and exposed to Kodak XAR-5 film. The primary antibodies (rabbit polyclonal; No. 931 for mouse SREBP-1a and -1c, No. 772 for SREBP-1c, which does not bind to SREBP-1a, and No. 528 for SREBP-2) were used as described previously (11, 17, 24). The precursor and mature SREBP-1 bands are ~125 and 65 kDa, respectively.

Transfection and luciferase assays

An expression plasmid for the human nuclear form of SREBP-1c constructed in pcDNA3.1(+) (Invitrogen) was described previously (25). Luciferase reporter plasmids for the SRE promoter (SRE-Luc) and the fatty acid synthase gene promoter (FAS-Luc) were prepared as described previously (8, 24). Human hepatoma HepG2 cells were cultured in DMEM containing 25 mM glucose, 100 U/ml penicillin, and 100 μg/ml streptomycin sulfate supplemented with 10% FBS. On day 0, cells were plated on a 12-well plate at 4.5×10^4 cells/well. On day 2, the indicated amounts of mature SREBP-1c expression plasmids, mock plasmids [empty pcDNA3.1(+)] to adjust total DNA amount, and luciferase reporter plasmids (FAS-Luc or SRE-Luc; 0.25 μg each) mixed with an SV-β-galactosidase reference plasmid (0.1 μg; p-SV-β-gal; Promega) were cotransfected into HepG2 cells using SuperFect Transfection Reagent (Qiagen) according to the manufacturer's protocol. The luciferase activity in transfectants was measured on a luminometer and normalized to β-galactosidase activity measured by standard kits (Promega).

3T3-L1 adipocytes were transfected by electroporation as described previously (26, 27). In brief, after cells became confluent (day 0), adipose conversion was induced in DMEM containing 25 mM glucose, 10% FBS, 0.5 mM isobutylmethylxanthine, 5 μg/ml bovine insulin, 0.25 μM dexamethasone, 1 μM pioglitazone, 33 μM biotin (Wako), 17 μM pantothenate (Wako), and antibiotics. After 48 h, the induction medium was removed and replaced by DMEM containing 25 mM glucose, 10% FBS, insulin, pioglitazone, biotin, and pantothenate. This medium was changed every 2 days. The adipocytes at day 8 of differentiation grown on 60 mm dishes were detached from dishes with 0.25% trypsin and 0.5 mg/ml collagenase (Wako) in PBS, washed twice, and resuspended in PBS. The indicated amounts of SREBP-1c expression plasmids, mock plasmids to adjust total DNA amount, luciferase reporter plasmids (FAS-Luc or SRE-Luc; 15 μg each), and control plasmids (pSV-β-gal; 10 μg) were cotransfected to

the cells by a pulse current generated from the electroporator (Cell-Porator; Invitrogen) at 160 V with 880 μF capacitance and a low ohm setting. After electroporation, cells were immediately mixed with fresh medium for 10 min before being reseeded onto 24-well collagen-coated plates and assayed at 40 h after transfection.

ChIP assays

ChIP assays were performed as described by Boyd and Farnham (28) with minor modifications. The supernatant of soluble chromatin derived from 1×10^7 cells was used. Briefly, rat primary hepatocytes and adipocytes were treated with 1% formaldehyde for 10 min. The cross-linking reaction was stopped by the addition of glycine to a final concentration of 0.125 M for 5 min. After washing with cold PBS, the cells were suspended in cell lysis buffer containing 10 mM HEPES at pH 7.9, 10 mM KCl, 1.5 mM $MgCl_2$, 1 mM EDTA, 1 mM EGTA, 0.5% Nonidet P-40, and protease inhibitors. After incubation for 30 min on ice, the cells were passed through a 26 gauge needle 20 times on ice. The nuclei were collected by microcentrifugation at 5,000 rpm and resuspended in nuclear lysis buffer (50 mM Tris-HCl at pH 8.1, 1% SDS, 10 mM EDTA, and protease inhibitors) on ice for 10 min. Samples were sonicated with a Branson sonifier at power 2 for six 10 s pulses to an average DNA length of <2 kb and then microcentrifuged at 15,000 rpm for 10 min. The supernatant was diluted 10-fold with buffer containing 0.01% SDS, 16.7 mM Tris-HCl at pH 8.1, 1.1% Triton X-100, 1.2 mM EDTA, 167 mM NaCl, and protease inhibitors and precleared for 1.5 h with Protein G-Sepharose. The supernatant was incubated with normal rabbit IgG or anti-SREBP-1 antibody overnight at 4°C.

Samples were subsequently washed four times using wash buffer A (0.1% SDS, 1% Triton X-100, 2 mM EDTA, 150 mM NaCl, and 20 mM Tris-HCl at pH 8.1), wash buffer B (0.1% SDS, 1% Triton X-100, 2 mM EDTA, 500 mM NaCl, and 20 mM Tris-HCl at pH 8.1), wash buffer C (0.25 M LiCl, 1% Nonidet P-40, 1% deoxycholate, 1 mM EDTA, and 10 mM Tris-HCl at pH 8.1), and wash buffer D (1 mM EDTA and 10 mM Tris-HCl at pH 8.0) and were eluted by 30 min of incubation with 100 μl of elution buffer (1% SDS, 50 mM $NaHCO_3$, and 10 mM DTT). Then, NaCl was added at a final concentration of 0.3 M and RNA was removed by the addition of RNase A, and the samples were incubated at 65°C for 4 h to reverse the formaldehyde-induced cross-linking. Protein was digested by proteinase K in 2× PK buffer (20 mM Tris-HCl at pH 7.5, 10 mM EDTA, and 1% SDS) at 45°C for 2 h. The resulting chromatin DNA was further purified on silica beads (Wizard DNA Clean-Up System; Promega) and used as a template for PCR. Primers used to amplify FAS promoter regions were as follows: for the SRE/E-box site at −65 (−109 to +63 was amplified), 5′-GACGCTCATTGGCCTGG-3′ and 5′-CTCTGGAGGCAGACGACAAG-3′; for the SRE-1 site at −150 (−94 to −299 was amplified), 5′-AGGACAGAGATGAGGGCGTC-3′

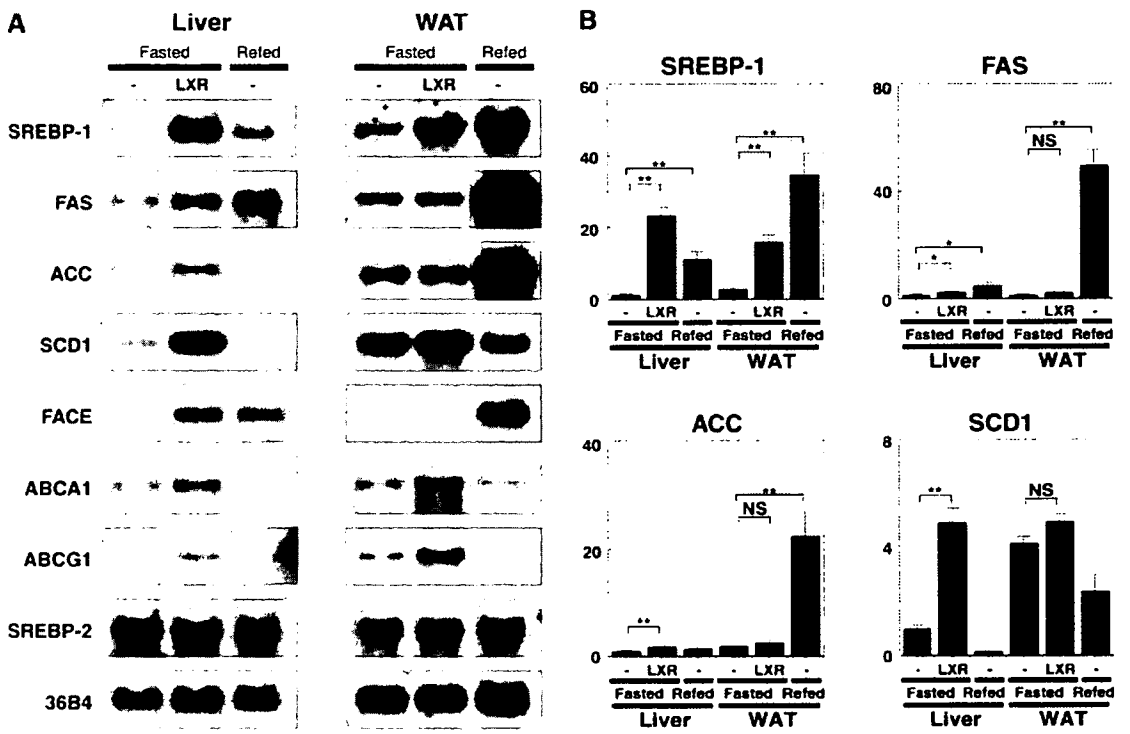

Fig. 1. Sterol regulatory element-binding protein (SREBP)-1c activation by liver X receptor (LXR) agonists does not increase lipogenic gene expression in mouse adipose tissue. Northern blot (A) and real-time PCR (B) analyses of liver and adipose tissue of mice treated with LXR agonist are shown. C57BL/6J mice (8 weeks old, male, four animals for each group) were treated with the LXR agonist T0901317 (50 mg/kg) as indicated and euthanized at 12 h after treatment in a 24 h fasted state. Refed control mice were refed for 12 h after 24 h of starvation. A: Total RNA (10 μg) pooled equally was subjected to Northern blotting. A cDNA probe for 36B4 (acidic ribosomal phosphoprotein P0) was used to confirm equal loading. B: Real-time PCR analysis of RNA isolated from liver and adipose tissue. mRNA levels of target genes were normalized to 36B4. Values are means ± SEM presented as fold changes relative to liver controls. ACC, acetyl-coenzyme A carboxylase; FACE, fatty acyl-coenzyme A elongase; SCD1, stearoyl-coenzyme A desaturase 1; WAT, white adipose tissue. * $P < 0.05$, ** $P < 0.01$ versus controls.

and 5'-CCAGGCCAATGAGCGTC-3'; for the nonspecific site (−1,076 to −904), 5'-AAGCCACTGCCCATAAGGTT-3' and 5'-TTAAAGGGAGGGAGGGTGAG-3'. For the SRE/E-box and nonspecific sites, PCR was performed using AmpliTaq Gold (Applied Biosystems) under the following reaction conditions: after 9 min at 95°C, 35 cycles of 1 min at 95°C, 30 s at 62°C, and 1 min at 72°C. For the SRE-1 site, PCR was performed using Advantage-GC Genomic Polymerase Mix (Clontech) under the following reaction conditions: after 1 min at 95°C, 35 cycles of 30 s at 94°C, 30 s at 62°C, and 2.5 min at 68°C. After amplification, PCR products were electrophoresed on a 3% NuSieve agarose gel and visualized by ethidium bromide staining. These experiments were performed at least three times.

RESULTS

SREBP-1c activation by LXR agonist does not induce lipogenic gene expression in adipose tissue

In our first series of experiments, we examined the effects of SREBP-1c overexpression on lipogenic gene expression in liver and adipose tissue. As expected, administration of synthetic LXR agonist T0901317 to animals (mice in **Fig. 1** and rats in **Fig. 2**) upregulated SREBP-1 expression and thereby the downstream lipogenic enzyme genes, such as FAS, ACC, and stearoyl-coenzyme A desaturase 1, in their livers. In contrast, quite unexpectedly, lipogenic genes in their adipose tissues were not influenced by the treatment, although SREBP-1 was markedly upregulated in the same way as in liver. These results from Northern blotting were confirmed by quantitative real-time PCR analyses (Fig. 1B). It is notable that SREBP-1 mRNA levels quantified by real-time PCR are equivalent in both tissues, as shown in Fig. 1B, denying the possibility that a lack of lipogenic gene induction in adipose tissue is a quantitative effect. The effect of LXR activation was further verified by the marked increase of ABCA1 and ABCG1, representatives of LXR-activated genes (29, 30), which were strongly induced in both tissues. These results were not altered by combined administration of both LXR agonist and the RXR agonist LG100268 (30 mg/kg), which produced additive effects on the SREBP-1 pathway in the liver but did not influence lipogenic gene expression in adipose tissue (data not shown).

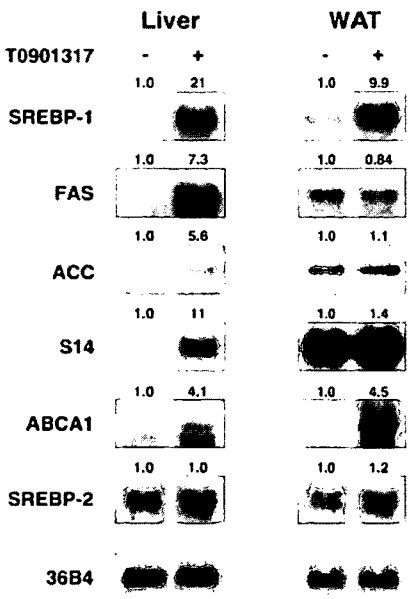

Fig. 2. SREBP-1c activation by LXR agonist does not induce lipogenic gene expression in rat adipose tissue. Northern blot analysis of liver and adipose tissue of rats treated with LXR agonist is shown. Wister rats (8 weeks old, male, three animals for each group) were administered the LXR agonist T0901317 (10 mg/kg) or vehicle alone and euthanized at 12 h after treatment in a fasted state. Total RNA (10 μg) pooled equally was subjected to Northern blotting. A cDNA probe for 36B4 was used to confirm equal loading. The quantification results were obtained with the BAS2000 system and normalized to the signal generated from 36B4 mRNA, and the fold changes against control are displayed above each blot. S14, Spot 14; WAT, white adipose tissue.

Posttranslational activation of SREBP-1 is intact, and mature protein is generated in adipose tissue

SREBP-1 is synthesized as a precursor bound to the endoplasmic reticulum and nuclear envelope and is released from the membrane into the nucleus as a mature protein by a cleavage process (6). Therefore, it is possible that defective posttranslational processing of SREBP-1 in adipocytes might result in this blunted response of lipogenic genes to SREBP-1 overexpression. To test this possibility, we separated nuclei from liver and adipose tissue and quantified the amount of mature SREBP-1 by immunoblot analysis. As shown in **Fig. 3**, nuclear contents of SREBP-1 were increased similarly by LXR agonist in both liver and adipose tissue, indicating that posttranslational processing of SREBP-1 is intact in adipose tissue (Fig. 3A, mice; Fig. 3B, rats). It was further confirmed by SREBP-1c-specific antibody that isoform 1c was increased in the nuclei of adipose tissue. These findings demonstrate that the defective response of lipogenic genes to SREBP-1 overexpression in adipose tissue is not attributable to an impairment of the SREBP-1c cleavage process.

To deny the possibility that the expression levels of the nuclear form of SREBP-1 protein in adipose tissue stimulated by LXR agonist are too low to increase lipogenic gene expression, the effect of T0901317 was compared with that of refeeding. As shown in Fig. 3C, the mature form of SREBP-1 in the nuclei of LXR-stimulated adipocytes is more abundant than that observed in adipocytes from refed animals. However, this abundant SREBP-1 protein of the active form did not induce FAS expression at all (Fig. 3D), demonstrating that the amount of SREBP-1 protein is not the cause of the inability of SREBP-1 to upregulate FAS expression in adipocytes.

SREBP-1 and lipogenic gene expression in primary cultured cells

LXR widely modifies lipid and glucose metabolism, affecting serum levels of insulin and fatty acids (31), which are known to influence the SREBP-1 pathway (32). To

JOURNAL OF LIPID RESEARCH

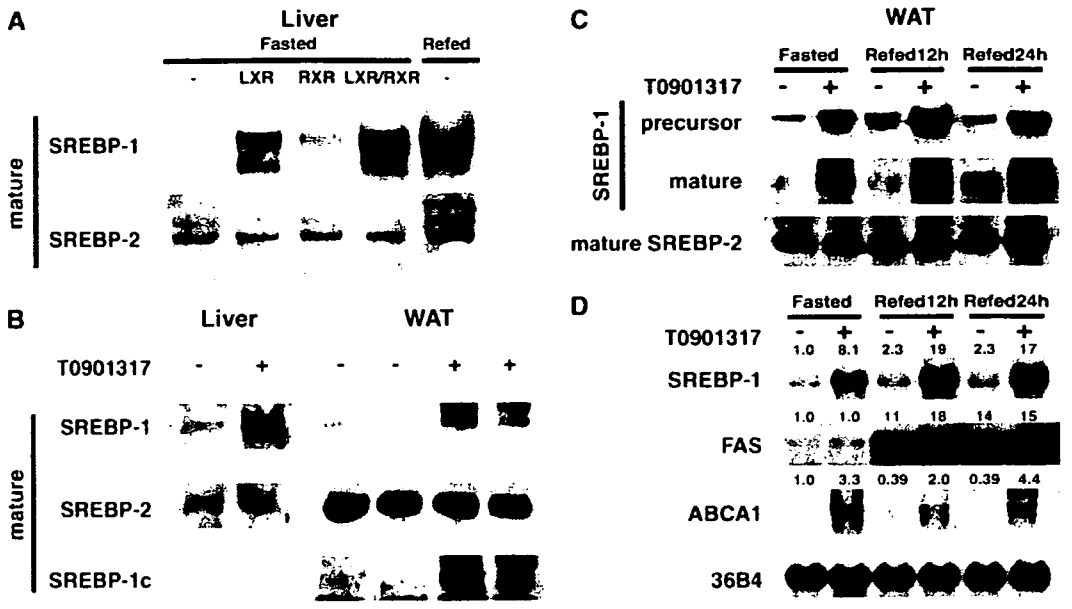

Fig. 3. Posttranslational activation of SREBP-1 is intact and mature protein is generated in adipose tissue. Immunoblot analyses of SREBPs in nuclear proteins from liver (A, B) and adipose tissue (B, C) are shown. A: Mature forms of SREBP-1 and -2 in the liver. C57BL/6J mice (8 weeks old, male, four mice for each group) were administered the LXR agonist T0901317 (50 mg/kg) and/or the retinoid X receptor (RXR) agonist LG100268 (30 mg/kg) as indicated and euthanized at 12 h after treatment in a 24 h fasted state. Refed control mice were refed for 12 h after 24 h of starvation. B: Mature forms of SREBP-1 and -2 in liver and adipose tissue were quantified from Wister rats (8 weeks old, male) administered T0901317 (10 mg/kg) or vehicle alone and euthanized at 12 h after treatment in a fasted state. Nuclei were isolated from liver (pooled within groups) and adipose tissue (individually), and aliquots of nuclear proteins (20 μg) were subjected to immunoblot analysis. SREBP-1c-specific antibody was also used. C, D: Effect of administering LXR agonist compared with that of refeeding rats. C: Precursor and mature forms of SREBP-1 in adipose tissue were visualized by immunoblots. D: Northern blotting of SREBP-1 and FAS. Wister rats (8 weeks old, male, three animals for each group) were administered T0901317 (10 mg/kg) or vehicle alone at 12 h before euthanization. WAT, white adipose tissue.

eliminate these indirect effects through systemic factors and reinforce the in vivo results, we also examined the effects of SREBP-1c activation in primary cultured hepatocytes and adipocytes in vitro, whose isoform patterns of SREBP-1 are 1c-predominant as assessed by quantitative real-time PCR assays (data not shown). In these primary models, it was demonstrated that the overexpression of SREBP-1 mRNA and thereby precursor proteins induced by LXR agonist led to the increase of mature SREBP-1 proteins in both hepatocytes and adipocytes (**Fig. 4**). However, the resulting activation of SREBP-1 produced totally different effects on lipogenic gene expression between hepatocytes and adipocytes; consistent with the in vivo results described above, FAS mRNA expression was upregulated by SREBP-1c in hepatocytes but was not induced in adipocytes.

Transcriptional activity of SREBP-1c for the FAS promoter is negligible in adipocytes

As described above, the contribution of SREBP-1 to lipogenic gene regulation was demonstrated to be different between hepatocytes and adipocytes. Because SREBP-1c activation processes are revealed to be equally intact in both cell types, it is presumed that nuclear SREBP-1 would have different transcriptional activity in hepatocytes and adipocytes. To test this hypothesis, we performed luciferase reporter gene assays and compared transcriptional activities of nuclear SREBP-1c between HepG2 hepatoma cells and 3T3-L1 adipocytes. We estimated the transcriptional activity of nuclear SREBP-1c against the FAS promoter by transfecting cells with FAS-Luc reporter plasmids along with mature SREBP-1c expression plasmids. Transfection efficiency was evaluated using an optimum SRE-Luc as a control. As shown in **Fig. 5**, in HepG2 cells, FAS-Luc and SRE-Luc were vigorously activated by SREBP-1c. In contrast, activation of FAS-Luc by the active form of SREBP-1c was faint in 3T3-L1 adipocytes, whereas SRE-Luc was highly activated. These data demonstrate that the transcriptional activity of SREBP-1c against the FAS promoter is far lower in adipocytes compared with hepatocytes.

SREBP-1 does not bind to the functional *cis* element on the FAS promoter in adipocytes

To further investigate the molecular mechanism against the inability of SREBP-1 to activate transcription from the FAS gene in adipocytes, we evaluated the direct binding of SREBP-1 to the FAS promoter using ChIP assays. In the FAS promoter, two potential binding sites for SREBP-1 have been identified: one is −65 SRE/E-box, which contains two tandem copies of SREs and the E-box; the other

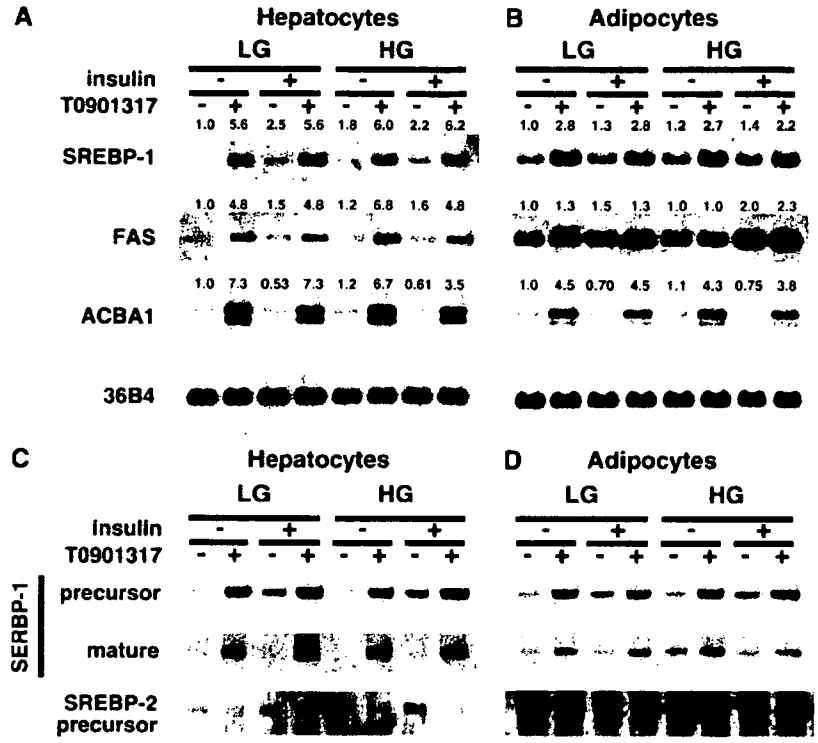

Fig. 4. Northern and Western blot analyses of SREBP-1 in primary hepatocytes and adipocytes. A, B: mRNA quantification of SREBP-1 and lipogenic genes in primary hepatocytes (A) and adipocytes (B). Hepatocytes isolated from rat livers (A) and adipocytes differentiated from rat preadipocytes (B) were incubated for 12 h with or without T0901317 (10 μM) and insulin (100 nM). Incubation medium contained either 5 mM glucose (LG; low glucose) or 25 mM glucose (HG; high glucose). Total RNA (10 μg) was subjected to Northern blotting. A cDNA probe for 36B4 was used to confirm equal loading. The quantification results were obtained with the BAS2000 system and normalized to the signal generated from 36B4 mRNA, and fold changes against control are displayed above each blot. C, D: Precursor and mature forms of SREBP-1 proteins from primary hepatocytes (C) and adipocytes (D) are shown. Cells were stimulated as described above, whole cell lysates (50 μg of protein) were subjected to immunoblot analysis, and the bands corresponding to precursor and mature SREBP-1 proteins are presented as indicated. These experiments were repeated twice, and reproducibility was confirmed.

is −150 SRE-1, which is not functional because of the lack of cofactor binding sites nearby, although the sequence itself is a complete SRE (5′-TCACCCCAC-3′) (33, 34). In our ChIP assays, SREBP-1 activation augmented its binding to −65 SRE/E-box in rat primary hepatocytes, as expected (**Fig. 6**). In sharp contrast to this, SREBP-1 activation did not result in its recruitment to −65 SRE/E-box in adipocytes, demonstrating that SREBP-1 does not bind to the functional *cis* element on the FAS promoter in adipocytes. Meanwhile, SREBP-1 activation led to its binding to −150 SRE-1 in both hepatocytes and adipocytes. These results were also confirmed using mouse primary cells (data not shown).

Genetic disruption of SREBP-1 decreases lipogenic gene expression as well as the responses to LXR activation in the liver, but not in adipose tissue

To further validate that SREBP-1 is not involved in the regulation of lipogenic genes in adipocytes, we evaluated FAS expression in SREBP-1 knockout mice with or without LXR stimulation. As shown in **Fig. 7**, genetic deletion of SREBP-1 impaired the transactivation of FAS in response to LXR activation in liver, whereas in adipose tissue, LXR activation did not alter the expression levels of these lipogenic genes in either SREBP-1 knockout or wild-type mice. These results demonstrate that SREBP-1 does not substantially contribute to the regulation of FAS expression in adipose tissue, whereas in the liver, SREBP-1 actually regulates the expression level of FAS.

DISCUSSION

This study has clearly demonstrated that lipogenic gene regulation is primarily independent of SREBP-1c in adipocytes. Hence, the involvement of SREBP-1c in fatty acid synthesis differs fundamentally between liver and adipose tissue, the two major lipogenic organs.

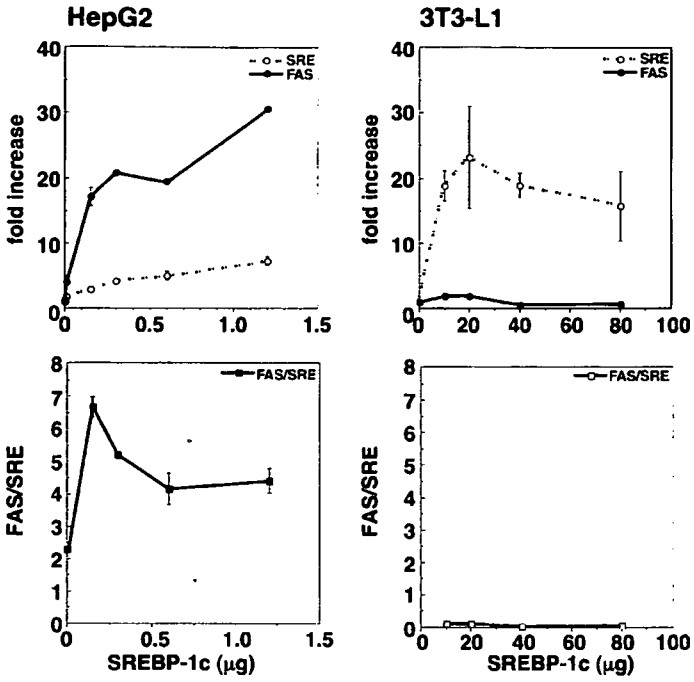

Fig. 5. Transcriptional activity of SREBP-1c against the FAS promoter is negligible in adipocytes. Transcriptional activities of the mature form of SREBP-1c in HepG2 hepatoma cells (left panels) and 3T3-L1 adipocytes (right panels) were measured by luciferase reporter gene assay. Both types of cells were transfected with the indicated amounts of mature SREBP-1c expression plasmids and mock plasmids [pcDNA3.1(+)] to adjust total DNA amount in combination with FAS-Luc or SRE-Luc and pSV-β-gal (note that transfection methods and scales are different between HepG2 and 3T3-L1 and that the amounts of transfected DNA cannot be compared between them). Luciferase activities were measured and normalized to β-galactosidase activities. In upper panels, values are expressed as fold changes against control (i.e., no SREBP-1c). Error bars represent SEM. These experiments were repeated twice, and reproducibility was confirmed.

Recently, a microarray analysis of mouse liver and adipose tissue stimulated by LXR agonist was reported by others (35). In that study, SREBP-1 mRNA expression was induced in both liver and adipose tissue by LXR agonist, whereas lipogenic genes such as fatty acid synthase, malic enzyme, and Spot 14 were upregulated only in liver and not in adipose tissue, supporting our data. We further proceeded to explore the underlying mechanism for this discrepancy and have revealed that the active form of SREBP-1 is definitely generated but does not transactivate lipogenic genes in adipocytes, as a result of defective binding to functional SRE in promoter regions in vivo.

In our first series of experiments, we demonstrated that in both adipocytes and hepatocytes the nuclear content of mature SREBP-1 protein parallels the amount of the precursor form of SREBP-1, whether its expression is increased by LXR activation or by refeeding. This observation indicates that the proteolytic activation of SREBP-1 precursor protein is intact in adipocytes and that SREBP-1 is basically activated when its mRNA expression is upregulated. This feature of SREBP-1 activation provides a sharp contrast to that of SREBP-2, which is tightly regulated through the cleavage processes as a pivotal part of the negative feedback system to maintain cholesterol homeostasis (6). In fact, SREBP-1 and -2 are reported to be regulated distinctly under some specific conditions (18, 36). It is intriguing that there is so much difference in the regulation of the proteolytic activation of SREBP-1 and -2, although they are both subject to the same cleavage machineries, consisting of SREBP cleavage-activating protein and site-1/2 proteases (37).

Nevertheless, in contrast to hepatocytes, increases of the active form of SREBP-1c protein failed to activate lipogenic genes in adipocytes. This ineffectiveness of SREBP-1c in adipocytes was validated by four lines of evidence: *1*) overexpression of active SREBP-1c had little effect on mRNA levels of lipogenic genes; *2*) transcriptional activity of SREBP-1c against the FAS promoter measured by reporter analysis was faint; *3*) nuclear SREBP-1c failed to bind to the functional *cis* element of the FAS promoter in adipocytes; and *4*) genetic disruption of SREBP-1 hardly affected mRNA levels of lipogenic genes. These results are further supported by the recent report claiming that mRNA levels of SREBP-1c do not coincide with the changes in adipose lipogenic gene expression (38, 39).

Regarding why mature SREBP-1c poorly transactivates lipogenic genes in adipocytes, there are two possibilities: *1*) SREBP-1c cannot reach its binding sites on the promoters; and *2*) SREBP-1c properly binds to its cognate sites, but the absence of required coactivator(s) or the presence of corepressor(s) specific to adipocytes prevents the genes from being transcribed. Our results from ChIP assays favor the former hypothesis. SREBP-1 was able to access both functional −65 SRE/E-box and nonfunctional −150 SRE-1 site in hepatocytes. In contrast, SREBP-1 could not bind to −65 SRE/E-box in adipocytes, although binding to −150 SRE-1 site was intact and similar to that observed in hepatocytes.

Another question our studies bring up is what transcription factors then regulate lipogenic gene expression in adipocytes. Unfortunately, we have few clues on this issue, except that this factor should be functionally activated by refeeding. Upstream stimulatory factors-1/2 (40–42), carbohydrate response element binding protein (43), and CCAAT/enhancer binding protein α (44) are potential candidates, but an as yet unknown

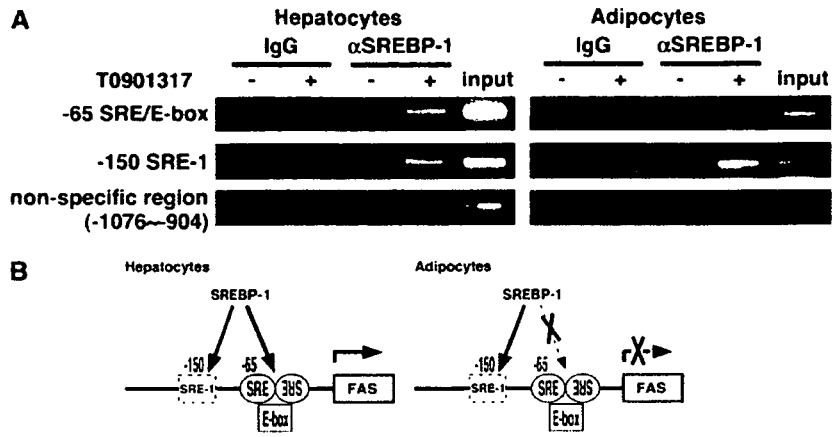

Fig. 6. SREBP-1 does not bind to the functional *cis* element on the FAS promoter in adipocytes. A: Chromatin immunoprecipitation (ChIP) assays using antibody to SREBP-1 and amplifying DNA fragments from the FAS promoter. Primary hepatocytes and adipocytes differentiated from preadipocytes were incubated for 12 h with or without T0901317 (10 μM). After cross-linking, the nuclei were isolated and sonicated, and chromatin protein-DNA complexes were immunoprecipitated with control rabbit IgG or anti-SREBP-1 antibodies. The resultant DNA was analyzed by PCR with primers amplifying −150 SRE-1, −65 SRE/E-box, and a nonspecific region (from −1,076 to −904) on the FAS promoter. The results shown here are representative of three independent experiments. B: Schematic representations of the FAS promoter. The FAS promoter contains two SREBP-1 recognition sites: −150 SRE-1 and −65 SRE/E-box. ChIP assays revealed tissue-dependent recruitment of SREBP-1; SREBP-1 can bind to both functional SRE/E-box and nonfunctional SRE-1 in hepatocytes, whereas the binding to SRE/E-box is prevented in adipocytes.

factor might be the answer. Further studies in adipocytes are imperative.

It has been reported by others that fatty acid synthase gene expression is increased by SREBP-1c through adenovirus-mediated gene transduction to 3T3-L1 adipocytes (45). In our experiments, FAS-Luc reporter activity was not increased by SREBP-1c transfection (Fig. 5). The cause of this discrepancy is not clear, but it is possible that the conditions of our transfection by electroporation method resulted in a more physiological level of SREBP-1c increase compared with adenovirus-mediated overexpression.

The importance of the LXR pathway in the regulation of lipogenesis and adipogenesis in adipocytes has been controversial; some reports have concluded that LXR stimulation leads to lipogenic gene activation (46, 47), whereas others have presented opposing data (35, 48). The current data support no impact of the LXR ligand on the gene expression of lipogenic enzymes, but the discrepancy

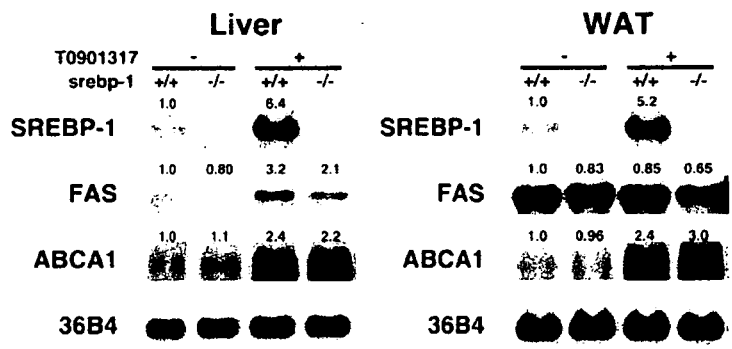

Fig. 7. Effects of the genetic disruption of SREBP-1. SREBP-1 disruption decreased lipogenic gene expression as well as the responses to LXR activation in the liver (left panel), whereas it did not do so in adipose tissue (right panel). SREBP-1 knockout mice in the C57BL/6J background (16 weeks old, female, three mice for each group) and their control littermates were treated with T0901317 (50 mg/kg) and analyzed by Northern blot. Mice were euthanized at 12 h after treatment in a 24 h fasted state. WAT, white adipose tissue.

might originate from differences in experimental conditions, such as variable glucose availability, that might indirectly influence lipogenesis, considering that the LXR pathway is reported to upregulate glucose transport (49). Our main conclusion here is that adipocyte lipogenesis is independent of SREBP-1c even if upregulated by LXR activation, consistent with our previous and current data from SREBP-1-null mice.

In summary, we have found that lipogenic genes in adipocytes are primarily regulated by factor(s) other than SREBP-1. Although proteolytic activation of SREBP-1 is intact and the resulting active form of SREBP-1 is upregulated whenever the SREBP-1 gene is stimulated, it does not function as a transactivator for lipogenic genes in adipocytes.

The authors thank Alyssa H. Hasty for critical reading of the manuscript. This work was supported by grants-in-aid from the Japan Health Sciences Foundation (to M.S.) and from the Ministry of Science, Education, Culture, and Technology of Japan (to N.Y., J-i.O., T.Y., N.Y., and H.S.). It was also supported by research grants from the Uehara Memorial Foundation, the ONO Medical Research Foundation, the Takeda Science Foundation, the Suzuken Memorial Foundation, the Japan Heart Foundation, the Kanae Foundation for the Promotion of Medical Science, the Senri Life Science Foundation, and the Okinaka Memorial Institute for Medical Research (to N.Y.).

REFERENCES

1. Goodridge, A. G. 1991. Fatty Acid Synthesis in Eucaryotes. Elsevier Science, Amsterdam, The Netherlands.
2. Goodridge, A. G. 1987. Dietary regulation of gene expression: enzymes involved in carbohydrate and lipid metabolism. *Annu. Rev. Nutr.* **7:** 157–185.
3. Shimomura, I., H. Shimano, B. S. Korn, Y. Bashmakov, and J. D. Horton. 1998. Nuclear sterol regulatory element-binding proteins activate genes responsible for the entire program of unsaturated fatty acid biosynthesis in transgenic mouse liver. *J. Biol. Chem.* **273:** 35299–35306.
4. Shimano, H., N. Yahagi, M. Amemiya-Kudo, A. H. Hasty, J. Osuga, Y. Tamura, F. Shionoiri, Y. Iizuka, K. Ohashi, K. Harada, et al. 1999. Sterol regulatory element-binding protein-1 as a key transcription factor for nutritional induction of lipogenic enzyme genes. *J. Biol. Chem.* **274:** 35832–35839.
5. Yokoyama, C., X. Wang, M. R. Briggs, A. Admon, J. Wu, X. Hua, J. L. Goldstein, and M. S. Brown. 1993. SREBP-1, a basic-helix-loop-helix-leucine zipper protein that controls transcription of the low density lipoprotein receptor gene. *Cell.* **75:** 187–197.
6. Brown, M. S., and J. L. Goldstein. 1997. The SREBP pathway: regulation of cholesterol metabolism by proteolysis of a membrane-bound transcription factor. *Cell.* **89:** 331–340.
7. Shimomura, I., H. Shimano, J. D. Horton, J. L. Goldstein, and M. S. Brown. 1997. Differential expression of exons 1a and 1c in mRNAs for sterol regulatory element binding protein-1 in human and mouse organs and cultured cells. *J. Clin. Invest.* **99:** 838–845.
8. Shimano, H., J. D. Horton, I. Shimomura, R. E. Hammer, M. S. Brown, and J. L. Goldstein. 1997. Isoform 1c of sterol regulatory element binding protein is less active than isoform 1a in livers of transgenic mice and in cultured cells. *J. Clin. Invest.* **99:** 846–854.
9. Horton, J. D., I. Shimomura, M. S. Brown, R. E. Hammer, J. L. Goldstein, and H. Shimano. 1998. Activation of cholesterol synthesis in preference to fatty acid synthesis in liver and adipose tissue of transgenic mice overproducing sterol regulatory element-binding protein-2. *J. Clin. Invest.* **101:** 2331–2339.
10. Yahagi, N., H. Shimano, A. H. Hasty, T. Matsuzaka, T. Ide, T. Yoshikawa, M. Amemiya-Kudo, S. Tomita, H. Okazaki, Y. Tamura, et al. 2002. Absence of sterol regulatory element-binding protein-1 (SREBP-1) ameliorates fatty livers but not obesity or insulin resistance in Lep(ob)/Lep(ob) mice. *J. Biol. Chem.* **277:** 19353–19357.
11. Sekiya, M., N. Yahagi, T. Matsuzaka, Y. Najima, M. Nakakuki, R. Nagai, S. Ishibashi, J. Osuga, N. Yamada, and H. Shimano. 2003. Polyunsaturated fatty acids ameliorate hepatic steatosis in obese mice by SREBP-1 suppression. *Hepatology.* **38:** 1529–1539.
12. Shimomura, I., R. E. Hammer, J. A. Richardson, S. Ikemoto, Y. Bashmakov, J. L. Goldstein, and M. S. Brown. 1998. Insulin resistance and diabetes mellitus in transgenic mice expressing nuclear SREBP-1c in adipose tissue: model for congenital generalized lipodystrophy. *Genes Dev.* **12:** 3182–3194.
13. Horton, J. D., I. Shimomura, S. Ikemoto, Y. Bashmakov, and R. E. Hammer. 2003. Overexpression of sterol regulatory element-binding protein-1a in mouse adipose tissue produces adipocyte hypertrophy, increased fatty acid secretion, and fatty liver. *J. Biol. Chem.* **278:** 36652–36660.
14. Repa, J. J., G. Liang, J. Ou, Y. Bashmakov, J. M. Lobaccaro, I. Shimomura, B. Shan, M. S. Brown, J. L. Goldstein, and D. J. Mangelsdorf. 2000. Regulation of mouse sterol regulatory element-binding protein-1c gene (SREBP-1c) by oxysterol receptors, LXRalpha and LXRbeta. *Genes Dev.* **14:** 2819–2830.
15. Yoshikawa, T., H. Shimano, M. Amemiya-Kudo, N. Yahagi, A. H. Hasty, T. Matsuzaka, H. Okazaki, Y. Tamura, Y. Iizuka, K. Ohashi, et al. 2001. Identification of liver X receptor-retinoid X receptor as an activator of the sterol regulatory element-binding protein 1c gene promoter. *Mol. Cell. Biol.* **21:** 2991–3000.
16. Mukherjee, R., P. J. Davies, D. L. Crombie, E. D. Bischoff, R. M. Cesario, L. Jow, L. G. Hamann, M. F. Boehm, C. E. Mondon, A. M. Nadzan, et al. 1997. Sensitization of diabetic and obese mice to insulin by retinoid X receptor agonists. *Nature.* **386:** 407–410.
17. Shimano, H., J. D. Horton, R. E. Hammer, I. Shimomura, M. S. Brown, and J. L. Goldstein. 1996. Overproduction of cholesterol and fatty acids causes massive liver enlargement in transgenic mice expressing truncated SREBP-1a. *J. Clin. Invest.* **98:** 1575–1584.
18. Sheng, Z., H. Otani, M. S. Brown, and J. L. Goldstein. 1995. Independent regulation of sterol regulatory element-binding proteins 1 and 2 in hamster liver. *Proc. Natl. Acad. Sci. USA.* **92:** 935–938.
19. Soukas, A., P. Cohen, N. D. Socci, and J. M. Friedman. 2000. Leptin-specific patterns of gene expression in white adipose tissue. *Genes Dev.* **14:** 963–980.
20. Osuga, J., S. Ishibashi, T. Oka, H. Yagyu, R. Tozawa, A. Fujimoto, F. Shionoiri, N. Yahagi, F. B. Kraemer, O. Tsutsumi, et al. 2000. Targeted disruption of hormone-sensitive lipase results in male sterility and adipocyte hypertrophy, but not in obesity. *Proc. Natl. Acad. Sci. USA.* **97:** 787–792.
21. Atkin, S. L., L. Hipkin, J. Radcliffe, and M. C. White. 1995. Hypotonic lysis of red blood cell contamination from human anterior pituitary adenoma cell preparations. *In Vitro Cell. Dev. Biol. Anim.* **31:** 657–658.
22. Horton, J. D., Y. Bashmakov, I. Shimomura, and H. Shimano. 1998. Regulation of sterol regulatory element binding proteins in livers of fasted and refed mice. *Proc. Natl. Acad. Sci. USA.* **95:** 5987–5992.
23. Hasty, A. H., H. Shimano, N. Yahagi, M. Amemiya-Kudo, S. Perrey, T. Yoshikawa, J. Osuga, H. Okazaki, Y. Tamura, Y. Iizuka, et al. 2000. Sterol regulatory element-binding protein-1 is regulated by glucose at the transcriptional level. *J. Biol. Chem.* **275:** 31069–31077.
24. Shimano, H., I. Shimomura, R. E. Hammer, J. Herz, J. L. Goldstein, M. S. Brown, and J. D. Horton. 1997. Elevated levels of SREBP-2 and cholesterol synthesis in livers of mice homozygous for a targeted disruption of the SREBP-1 gene. *J. Clin. Invest.* **100:** 2115–2124.
25. Yamamoto, T., H. Shimano, Y. Nakagawa, T. Ide, N. Yahagi, T. Matsuzaka, M. Nakakuki, A. Takahashi, H. Suzuki, H. Sone, et al. 2004. SREBP-1 interacts with hepatocyte nuclear factor-4 {alpha} and interferes with PGC-1 recruitment to suppress hepatic gluconeogenic genes. *J. Biol. Chem.* **279:** 12027–12035.
26. Min, J., S. Okada, M. Kanzaki, J. S. Elmendorf, K. J. Coker, B. P. Ceresa, L. J. Syu, Y. Noda, A. R. Saltiel, and J. E. Pessin. 1999. Synip: a novel insulin-regulated syntaxin 4-binding protein mediating GLUT4 translocation in adipocytes. *Mol. Cell.* **3:** 751–760.
27. Jiang, Z. Y., Q. L. Zhou, K. A. Coleman, M. Chouinard, Q. Boese, and M. P. Czech. 2003. Insulin signaling through Akt/protein kinase B analyzed by small interfering RNA-mediated gene silencing. *Proc. Natl. Acad. Sci. USA.* **100:** 7569–7574.
28. Boyd, K. E., and P. J. Farnham. 1999. Coexamination of site-specific transcription factor binding and promoter activity in living cells. *Mol. Cell. Biol.* **19:** 8393–8399.
29. Costet, P., Y. Luo, N. Wang, and A. R. Tall. 2000. Sterol-dependent

transactivation of the ABC1 promoter by the liver X receptor/retinoid X receptor. *J. Biol. Chem.* **275:** 28240–28245.
30. Repa, J. J., S. D. Turley, J. A. Lobaccaro, J. Medina, L. Li, K. Lustig, B. Shan, R. A. Heyman, J. M. Dietschy, and D. J. Mangelsdorf. 2000. Regulation of absorption and ABC1-mediated efflux of cholesterol by RXR heterodimers. *Science.* **289:** 1524–1529.
31. Steffensen, K. R., and J. A. Gustafsson. 2004. Putative metabolic effects of the liver X receptor (LXR). *Diabetes.* **53 (Suppl. 1):** 36–42.
32. Horton, J. D., J. L. Goldstein, and M. S. Brown. 2002. SREBPs: activators of the complete program of cholesterol and fatty acid synthesis in the liver. *J. Clin. Invest.* **109:** 1125–1131.
33. Bennett, M. K., J. M. Lopez, H. B. Sanchez, and T. F. Osborne. 1995. Sterol regulation of fatty acid synthase promoter. *J. Biol. Chem.* **270:** 25578–25583.
34. Kim, J. B., G. D. Spotts, Y. D. Halvorsen, H. M. Shih, T. Ellenberger, H. C. Towle, and B. M. Spiegelman. 1995. Dual DNA binding specificity of ADD1/SREBP1 controlled by a single amino acid in the basic helix-loop-helix domain. *Mol. Cell. Biol.* **15:** 2582–2588.
35. Stulnig, T. M., K. R. Steffensen, H. Gao, M. Reimers, K. Dahlman-Wright, G. U. Schuster, and J. A. Gustafsson. 2002. Novel roles of liver X receptors exposed by gene expression profiling in liver and adipose tissue. *Mol. Pharmacol.* **62:** 1299–1305.
36. Yahagi, N., H. Shimano, A. H. Hasty, M. Amemiya-Kudo, H. Okazaki, Y. Tamura, Y. Iizuka, F. Shionoiri, K. Ohashi, J. Osuga, et al. 1999. A crucial role of sterol regulatory element-binding protein-1 in the regulation of lipogenic gene expression by polyunsaturated fatty acids. *J. Biol. Chem.* **274:** 35840–35844.
37. Brown, M. S., and J. L. Goldstein. 1999. A proteolytic pathway that controls the cholesterol content of membranes, cells, and blood. *Proc. Natl. Acad. Sci. USA.* **96:** 11041–11048.
38. Palmer, D. G., G. A. Rutter, and J. M. Tavare. 2002. Insulin-stimulated fatty acid synthase gene expression does not require increased sterol response element binding protein 1 transcription in primary adipocytes. *Biochem. Biophys. Res. Commun.* **291:** 439–443.
39. Bertile, F., and T. Raclot. 2004. mRNA levels of SREBP-1c do not coincide with the changes in adipose lipogenic gene expression. *Biochem. Biophys. Res. Commun.* **325:** 827–834.
40. Casado, M., V. S. Vallet, A. Kahn, and S. Vaulont. 1999. Essential role in vivo of upstream stimulatory factors for a normal dietary response of the fatty acid synthase gene in the liver. *J. Biol. Chem.* **274:** 2009–2013.
41. Latasa, M-J., Y. S. Moon, K-H. Kim, and H. S. Sul. 2000. Nutritional regulation of the fatty acid synthase promoter in vivo: sterol regulatory element binding protein functions through an upstream region containing a sterol regulatory element. *Proc. Natl. Acad. Sci. USA.* **97:** 10619–10624.
42. Latasa, M-J., M. J. Griffin, Y. S. Moon, C. Kang, and H. S. Sul. 2003. Occupancy and function of the −150 sterol regulatory element and −65 E-box in nutritional regulation of the fatty acid synthase gene in living animals. *Mol. Cell. Biol.* **23:** 5896–5907.
43. Yamashita, H., M. Takenoshita, M. Sakurai, R. K. Bruick, W. J. Henzel, W. Shillinglaw, D. Arnot, and K. Uyeda. 2001. A glucose-responsive transcription factor that regulates carbohydrate metabolism in the liver. *Proc. Natl. Acad. Sci. USA.* **98:** 9116–9121.
44. Matsusue, K., O. Gavrilova, G. Lambert, H. B. Brewer, Jr., J. M. Ward, Y. Inoue, D. LeRoith, and F. J. Gonzalez. 2004. Hepatic CCAAT/enhancer binding protein alpha mediates induction of lipogenesis and regulation of glucose homeostasis in leptin-deficient mice. *Mol. Endocrinol.* **18:** 2751–2764.
45. Lay, S. L., I. Lefrere, C. Trautwein, I. Dugail, and S. Krief. 2002. Insulin and sterol-regulatory element-binding protein-1c (SREBP-1C) regulation of gene expression in 3T3-L1 adipocytes. Identification of CCAAT/enhancer-binding protein beta as an SREBP-1c target. *J. Biol. Chem.* **277:** 35625–35634.
46. Juvet, L. K., S. M. Andresen, G. U. Schuster, K. T. Dalen, K. A. Tobin, K. Hollung, F. Haugen, S. Jacinto, S. M. Ulven, K. Bamberg, et al. 2003. On the role of liver X receptors in lipid accumulation in adipocytes. *Mol. Endocrinol.* **17:** 172–182.
47. Seo, J. B., H. M. Moon, W. S. Kim, Y. S. Lee, H. W. Jeong, E. J. Yoo, J. Ham, H. Kang, M. G. Park, K. R. Steffensen, et al. 2004. Activated liver X receptors stimulate adipocyte differentiation through induction of peroxisome proliferator-activated receptor gamma expression. *Mol. Cell. Biol.* **24:** 3430–3444.
48. Ross, S. E., R. L. Erickson, I. Gerin, P. M. DeRose, L. Bajnok, K. A. Longo, D. E. Misek, R. Kuick, S. M. Hanash, K. B. Atkins, et al. 2002. Microarray analyses during adipogenesis: understanding the effects of Wnt signaling on adipogenesis and the roles of liver X receptor alpha in adipocyte metabolism. *Mol. Cell. Biol.* **22:** 5989–5999.
49. Laffitte, B. A., L. C. Chao, J. Li, R. Walczak, S. Hummasti, S. B. Joseph, A. Castrillo, D. C. Wilpitz, D. J. Mangelsdorf, J. L. Collins, et al. 2003. Activation of liver X receptor improves glucose tolerance through coordinate regulation of glucose metabolism in liver and adipose tissue. *Proc. Natl. Acad. Sci. USA.* **100:** 5419–5424.

Original Article

Involvement of Apolipoprotein E in Excess Fat Accumulation and Insulin Resistance

Junhong Gao,[1,2] Hideki Katagiri,[2] Yasushi Ishigaki,[1] Tetsuya Yamada,[1] Takehide Ogihara,[2] Junta Imai,[1,2] Kenji Uno,[1,2] Yutaka Hasegawa,[1,2] Makoto Kanzaki,[3] Tokuo T. Yamamoto,[4] Shun Ishibashi,[5] and Yoshitomo Oka[1]

Although apolipoprotein E (apoE) is well known to play a major role in lipid metabolism, its role in glucose and energy homeostasis remains unclear. Herein, we established apoE-deficient genetically obese Ay (apoE$^{-/-}$;Ay/+) mice. ApoE deficiency in Ay mice prevented the development of obesity, with decreased fat accumulation in the liver and adipose tissues. ApoE$^{-/-}$;Ay/+ mice exhibited better glucose tolerance than apoE$^{+/+}$;Ay/+ mice. Insulin tolerance testing and hyperinsulinemic-euglycemic clamp study revealed marked improvement of insulin sensitivity, despite increased plasma free fatty acid levels. These metabolic phenotypes were reversed by adenoviral replenishment of apoE protein, indicating circulating apoE to be involved in increased adiposity and obesity-related metabolic disorders. Uptake of apoE-lacking VLDL into the liver and adipocytes was markedly inhibited, but adipocytes in apoE$^{-/-}$;Ay/+ mice exhibited normal differentiation, suggesting that apoE-dependent VLDL transport is involved in the development of obesity, i.e., surplus fat accumulation. Interestingly, apoE$^{-/-}$;Ay/+ mice exhibited decreased food intake and increased energy expenditure. Pair-feeding experiments indicate these phenomena to both contribute to the obesity-resistant phenotypes associated with apoE deficiency. Thus, apoE is involved in maintaining energy homeostasis. ApoE-dependent excess fat accumulation is a promising therapeutic target for the metabolic syndrome. ***Diabetes*** **56:24–33, 2007**

From the [1]Division of Molecular Metabolism and Diabetes, Tohoku University Graduate School of Medicine, Sendai, Japan; the [2]Division of Advanced Therapeutics for Metabolic Diseases, Center for Translational and Advanced Animal Research, Tohoku University Graduate School of Medicine, Sendai, Japan; the [3]Tohoku University Bio-Engineering Research Organization, Sendai, Japan; the [4]Center for Advanced Genome Research, Institute of Development, Aging and Cancer, Tohoku University, Sendai, Japan; and the [5]Division of Endocrinology and Metabolism, Department of Medicine, Jichi Medical School, Tochigi, Japan.

Address correspondence and reprint requests to Hideki Katagiri, MD, PhD, Division of Advanced Therapeutics for Metabolic Diseases, Center for Translational and Advanced Animal Research, Tohoku University Graduate School of Medicine, 2-1 Seiryo-machi, Aoba-ku, Sendai 980-8575, Japan. E-mail: katagiri@mail.tains.tohoku.ac.jp.

Received for publication 1 February 2006 and accepted in revised form 16 October 2006.

J.G., H.K., and Y.I. contributed equally to this work.

Additional information for this article can be found in an online appendix at http://diabetes.diabetesjournals.org.

ApoE, apolipoprotein E; FFA, free fatty acid; HPLC, high-performance liquid chromatography; IRS, insulin receptor substrate; TNF, tumor necrosis factor; VLDLR, VLDL receptor.

DOI: 10.2337/db06-0144

Obesity causes various metabolic disorders, including diabetes, dyslipidemia, and hypertension and has become a major public health concern in most industrialized countries in recent decades (1). Obesity results mainly from excess energy intake and physical inactivity, and the molecular mechanisms of body weight control have been intensively studied from various aspects, including appetite, energy expenditure, glucose and lipid metabolism, and adiposity (2). Excess fat accumulation is associated with metabolic disorders including insulin resistance, glucose intolerance, and dyslipidemia (3). In addition, we reported that dissipating excess energy improves diabetes and obesity in mice (4). On the other hand, lipoatrophy also leads to these metabolic disorders in mice and humans. Fat-less mice (5,6) as well as patients with lipodystrophy (7) exhibit severe insulin resistance and diabetes. Thus, having an appropriate adipose tissue amount is important for maintaining glucose homeostasis via adipocyte metabolic activities including production and secretion of adipocytokines.

Apolipoprotein E (apoE) is a structural component of all lipoprotein particles except LDL and serves as a high-affinity ligand for lipoprotein receptors (8). ApoE plays important roles in hepatic uptake of chylomicron and VLDL remnants (9,10) as well as hepatic secretion of VLDL (11). In contrast, involvement of apoE in adiposity, insulin sensitivity, and glucose metabolism is somewhat controversial. ApoE$^{-/-}$ mice treated with gold thioglucose become obese and diabetic (12). High-fat chow induces obesity in apoE$^{-/-}$ mice in a manner similar to that in wild-type C57BL/6 mice, while apoE deficiency produced resistance to some obesity-related phenotypic features, including hyperinsulinemia and hyperglycemia (13). On the other hand, Chiba et al. reported that apoE deficiency in *ob/ob* mice resulted in neither increased body weight nor adiposity, but glucose metabolism and insulin sensitivity were not examined (14). They attributed decreased adiposity in *ob/ob*;apoE$^{-/-}$ mice to impaired adipocyte differentiation based on in vitro findings obtained using bone marrow stromal cells and 3T3-L1 cells. However, impaired adipocyte differentiation induces severe insulin resistance and diabetes (5,6), markedly different from the metabolic phenotypes of apoE$^{-/-}$ mice. Thus, it remains unclear how, and even whether, apoE is involved in adiposity and glucose metabolism.

Herein, we recognized that adult apoE$^{-/-}$ mice are leaner and more glucose tolerant than wild-type mice. In contrast, younger apoE$^{-/-}$ mice exhibit normal adiposity,

i.e., they are not lipoatrophic. These findings led us to postulate that apoE is involved in surplus fat accumulation, resulting in the development of insulin resistance, but does not play a major role in the fat accumulation required for adipocyte function. To clarify whether apoE is involved in the development of insulin resistance associated with obesity and, if so, to identify the underlying mechanisms, we established apoE-deficient genetically obese Ay (apoE$^{-/-}$;Ay/+) mice. Without impairing adipocyte differentiation in vivo, apoE deficiency in Ay mice prevented obesity, glucose intolerance, and insulin resistance. Interestingly, apoE$^{-/-}$;Ay/+ mice exhibited decreased food intake and increased energy expenditure, both of which contribute to the obesity-resistant phenotypes associated with apoE deficiency. Thus, apoE is a key molecule for development of obesity, i.e., excess fat accumulation, and is a possible therapeutic target for the metabolic syndrome.

RESEARCH DESIGN AND METHODS

Animal studies were conducted in accordance with the institutional guidelines for animal experiments at Tohoku University. ApoE$^{+/-}$;Ay/+ mice were obtained by mating male KKAy mice (Nippon CLEA, Shizuoka, Japan) and female apoE-deficient mice with the C57BL/6J background (15) (The Jackson Laboratory, Bar Harbor, ME). Male apoE$^{+/-}$;Ay/+ mice were mated with female apoE$^{+/-}$ mice with the C57BL/6J background. Mice of three genotyopes, apoE$^{+/+}$;Ay/+, apoE$^{+/-}$;Ay/+, and apoE$^{-/-}$;Ay/+, were selected. Littermates were used in each experiment. These mice were housed individually and started on a high-fat diet consisting of 15.3% (wt/wt) fat (Quick Fat; Nippon CLEA, Shizuoka, Japan) at 6 weeks of age. Experiments were performed 5 weeks after high-fat loading. Viruses were administered intravenously at a dose of 2×10^8 plaque-forming units 4 weeks after high-fat loading. For pair-feeding experiments, apoE$^{+/+}$;Ay/+ mice were allotted into two groups at 4 weeks of age. One group was given their daily food allotments based on the previous days' consumption by apoE$^{-/-}$;Ay/+ littermate mice.

Recombinant adenovirus preparation. Recombinant adenovirus, containing the human apoE2, E3, E4, or bacterial β-galactosidase gene (*Adex1CAlacZ*) cDNA under the CAG promoter, was prepared as described previously (16).

Oxygen consumption. Oxygen consumption was measured with an O_2/CO_2 metabolism measuring system (model MK-5000RQ; Muromachikikai, Tokyo, Japan) as described previously (4).

Histological analysis. Livers and adipose tissues were removed, fixed with 10% formalin, and embedded in paraffin. Tissue sections were stained with hematoxylin-eosin or 0.1% (wt/vol) Oil Red O. Total adipocyte areas were traced manually and analyzed. Brown and white adipocyte areas were measured in 100 or more cells per mouse in each group.

Triglyceride contents of the liver and adipose tissue. Frozen livers or adipose tissues were homogenized, and triglycerides were extracted with $CHCl_3$:CH_3OH (2:1 vol:vol), dried, and resuspended in 2-propanol. Triglyceride contents were measured using Lipidos liquid (Toyobo, Osaka, Japan).

Tyrosine phosphorylation of insulin receptor substrate 1. Mice that had been fasted for 16 h were injected with 100 μl normal saline (0.9% NaCl), with or without 10 units/kg body wt of insulin via the tail vein. Hindlimb muscles were removed 300 s later and immediately homogenized. After centrifugation, the resulting supernatants were used for immunoprecipitation with anti–insulin receptor substrate 1 (IRS-1) antibody (17). Immunoprecipitates were subjected to SDS-PAGE and then immunoblotted using antiphosphotyrosine antibody (4G10) as described previously (17).

Blood analysis. Blood glucose, plasma insulin, leptin, adiponectin, tumor necrosis factor (TNF)-α, total cholesterol, triglyceride, and free fatty acid (FFA) concentrations were determined as described previously (4). Plasma lipoproteins were analyzed by high-performance liquid chromatography (HPLC) using molecular sieve columns (Skylight Biotech, Akita, Japan) (18).

Glucose and insulin tolerance tests. Glucose and insulin tolerance tests were performed as described previously with slight modification (19). Glucose tolerance tests were performed on fasted (10 h) mice. Mice were given oral glucose (1 g/kg body wt), and blood glucose was assayed immediately before and at 15, 30, 60, and 120 min postadministration. Insulin tolerance tests were performed on fed mice. Mice were injected with human regular insulin (1.5 units/kg body wt; Eli Lilly, Kobe, Japan) into the intraperitoneal space, and blood glucose was assayed immediately before and at 20, 40, 60, and 80 min postinjection.

Hyperinsulinemic-euglycemic clamp. Hyperinsulinemic-euglycemic clamp studies were performed as described previously (20). Chronically cannulated, conscious and unrestrained mice were fasted for 6 h before the study. Insulin (500 mU · kg^{-1} · min^{-1}) was infused throughout the clamp study. Blood glucose was monitored every 5 min via carotid arterial catheter samples. Glucose was infused at a variable rate to maintain blood glucose at 120 mg/dl. The glucose infusion rate and endogenous glucose production were calculated as described (20).

Quantitative RT-PCR–based gene expression. Total RNA was isolated from 0.1 g mouse adipose tissue with Isogen (Wako Pure Chemical, Osaka, Japan), and cDNA was synthesized with a Cloned AMV First Strand Synthesis Kit (Invitrogen, Rockville, MD) using 5 μg total RNA. cDNA synthesized from total RNA was evaluated using real-time quantitative PCR (Light Cycler Quick System 350S; Roche Diagnostics, Mannheim, Germany). The relative amount of mRNA was calculated with 28S rRNA as the invariant control. The primers used are described in Supplemental Table 1 (online appendix [available at http://diabetes.diabetesjournals.org]).

β-VLDL uptake into cultured adipocytes. Murine 3T3-L1 preadipocytes were maintained and differentiated into adipocytes as described previously (21). β-VLDL ($d < 1.006$ g/ml) was purified from the blood of apoE$^{-/-}$ mice with high-fat loading and labeled with fluorescent lipid DiI (1,1′-dioctadecyl-3,3,3′,3′-tetramethylindocarbocyanine perchlorate) as described previously (22). After labeling with DiI, β-VLDL was incubated with an equal amount of recombinant human apoE3 for 1 h at 37°C (23). DiI-labeled β-VLDL (4 μg protein/ml) with or without apoE had been incubated with fully differentiated 3T3-L1 adipocytes for 8 h at 37°C. Cells were rinsed twice with PBS and solubilized with 0.1 N NaOH/1% SDS. Fluorescent intensities of cell lysates were measured with a fluorescent spectrophotometer (F-2000; Hitachi, Tokyo, Japan) (24).

Triglyceride secretion rate. To assess hepatic triglyceride secretion, 500 mg/kg Triton WR-1339 (Sigma), which blocks lipolysis of triglycerides in peripheral tissue, was injected into the tail veins of the 6 h–fasted apoE$^{+/+}$; Ay/+ mice, and blood samples were taken immediately before and 30, 60, and 90 min after injection (25).

Hepatic uptake of β-VLDL. Male C57BL/6N mice at 6 weeks of age were injected via tail vein with fluorescent β-VLDL (5 μg/mouse) with or without apoE in 0.2 ml PBS. Thirty minutes after injection, the mice were killed and their livers excised for lipid extraction and fluorescence measurement as described previously (26).

Statistical analysis. All data were expressed as means ± SEM. The statistical significance of differences was assessed by the unpaired *t* test and one-factor ANOVA.

RESULTS

ApoE deficiency inhibited the development of obesity. This study was prompted by the unexpected observation that aged apoE$^{-/-}$ mice are leaner and more insulin sensitive than apoE$^{+/+}$ mice of the same age with the C57BL/6J background. Therefore, we weighed apoE$^{-/-}$ and apoE$^{+/+}$ mice from 6 to 42 weeks of age, while maintaining the animals on high-fat chow. Body weights were similar through 10 weeks of age, but apoE$^{-/-}$ mice had significantly lower body weights after 14 weeks of age (Fig. 1*A*). Glucose tolerance in 30-week-old apoE$^{-/-}$ mice was moderately better than that in apoE$^{+/+}$ littermate mice (Fig. 1*B*). Thus, apoE deficiency prevents the development of obesity and associated glucose intolerance, while its effects on glucose tolerance are small.

Next, to elucidate the roles of apoE in development of the metabolic disorders associated with obesity, we established apoE$^{+/+}$;Ay/+, apoE$^{+/-}$;Ay/+, and apoE$^{-/-}$;Ay/+ mice. These mice were fed a 15% fat chow from 6 weeks of age. First, we compared body weights. As shown in Fig. 1*C*, mice gained weight in an apoE gene dosage-dependent manner; apoE deficiency significantly suppressed weight gain. Several organs and tissues were weighed at 11 weeks of age. Weights of the liver and both brown and white adipose tissues were significantly lower in an apoE gene dosage-dependent manner (Fig. 1*D*). In contrast, weights of other organs, which are minimally involved in lipid accumulation, were similar in apoE$^{+/+}$;Ay/+ and apoE$^{-/-}$; Ay/+ mice (Supplemental Table 2 [online appendix]). Triglyceride contents of the liver and mesenteric adipose

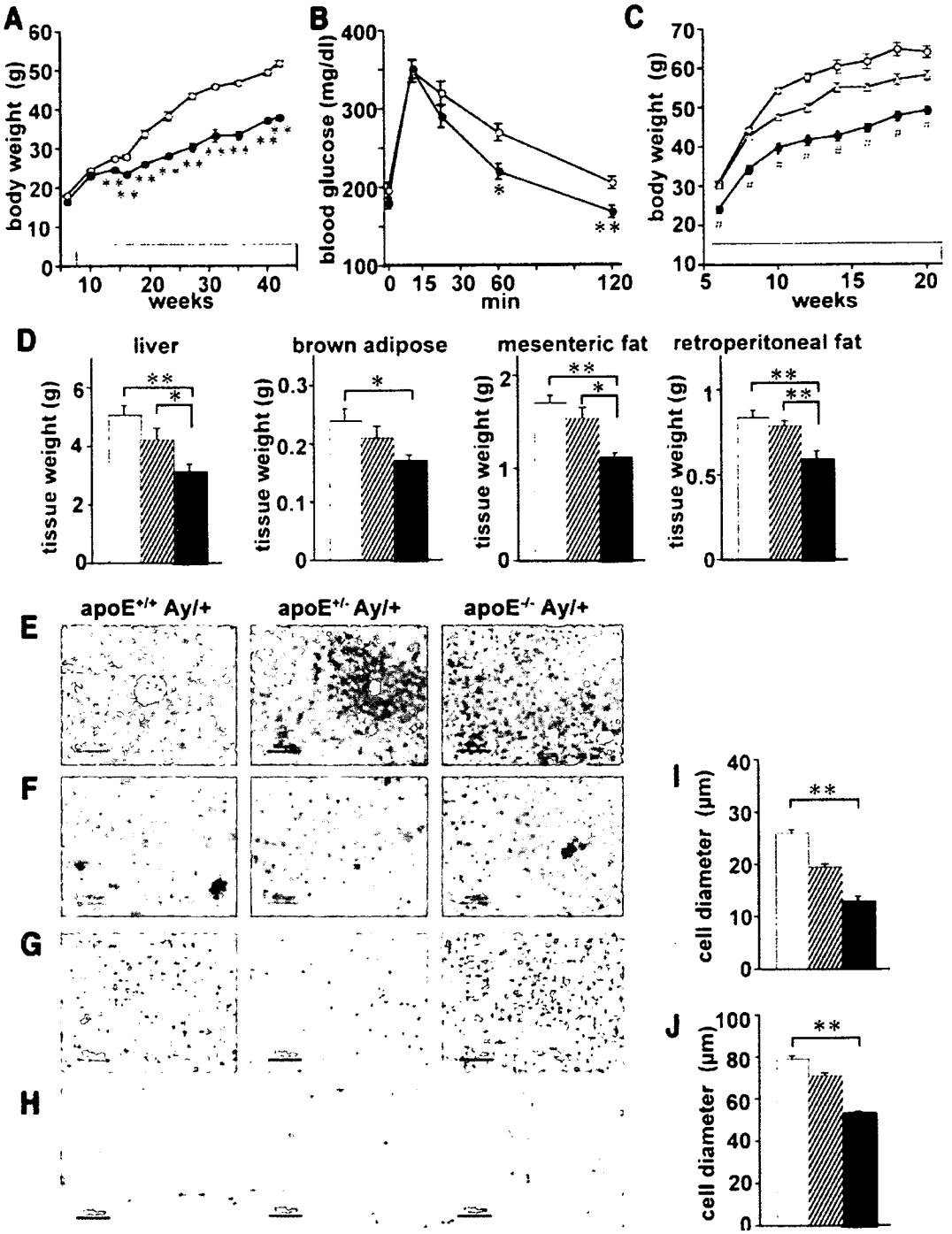

FIG. 1. ApoE deficiency suppressed body weight gain and fat accumulation. *A* and *B*: Body weights were determined from 6 to 40 weeks of age (*A*) and glucose tolerance tests were performed (*B*) in apoE$^{+/+}$ mice (○) and apoE$^{-/-}$ mice (●; n = 6 per group) at 30 weeks of age with the C57BL/6 background. *C*: Body weights were determined from 6 to 20 weeks of age in apoE$^{+/+}$;Ay/+ (○), apoE$^{+/-}$;Ay/+ (△), and apoE$^{-/-}$;Ay/+ (●) mice fed 15% fat chow. *D*–*J*: The liver and fat tissues of apoE$^{+/+}$;Ay/+, apoE$^{+/-}$;Ay/+, and apoE$^{-/-}$;Ay/+ mice at 11 weeks of age. *D*: The liver, brown adipose, and mesenteric and retroperitoneal white adipose tissues from apoE$^{+/+}$;Ay/+ (□), apoE$^{+/-}$;Ay/+ (▨), and apoE$^{-/-}$;Ay/+ (■) mice (n = 6–8 per group) were weighed. *E*–*J*: Histological findings of the liver stained with hematoxylin-eosin (*E*) and Oil Red O (*F*), as well as hematoxylin-eosin staining of brown adipose (*G*) and mesenteric white adipose (*H*) tissues in apoE$^{+/+}$;Ay/+ (*left*), apoE$^{+/-}$;Ay/+ (*middle*), and apoE$^{-/-}$;Ay/+ (*right*) mice. Brown adipose (*I*) and mesenteric white adipose (*J*) cell diameters were measured in apoE$^{+/+}$;Ay/+ (□), apoE$^{+/-}$;Ay/+ (▨), and apoE$^{-/-}$;Ay/+ (□) mice. Representative histological findings are shown. Data are presented as means ± SE. *P < 0.05, **P < 0.01 by the unpaired t test and one-way ANOVA.

tissue were significantly smaller in apoE$^{-/-}$;Ay/+ than in apoE$^{+/+}$;Ay/+ mice (apoE$^{+/+}$;Ay/+ vs. apoE$^{-/-}$;Ay/+ mice: liver, 0.467 ± 0.069 vs. 0.365 ± 0.036 mg/protein, P = 0.02; white adipose tissue, 12.4 ± 1.4 vs. 5.8 ± 1.3 mg/protein, P = 0.002). Histological analyses revealed that apoE deficiency inhibited hepatic fat accumulation, while abundant lipid droplets were present in the livers of apoE$^{+/+}$;Ay/+ mice (Fig. 1*E* and *F*). In addition, brown

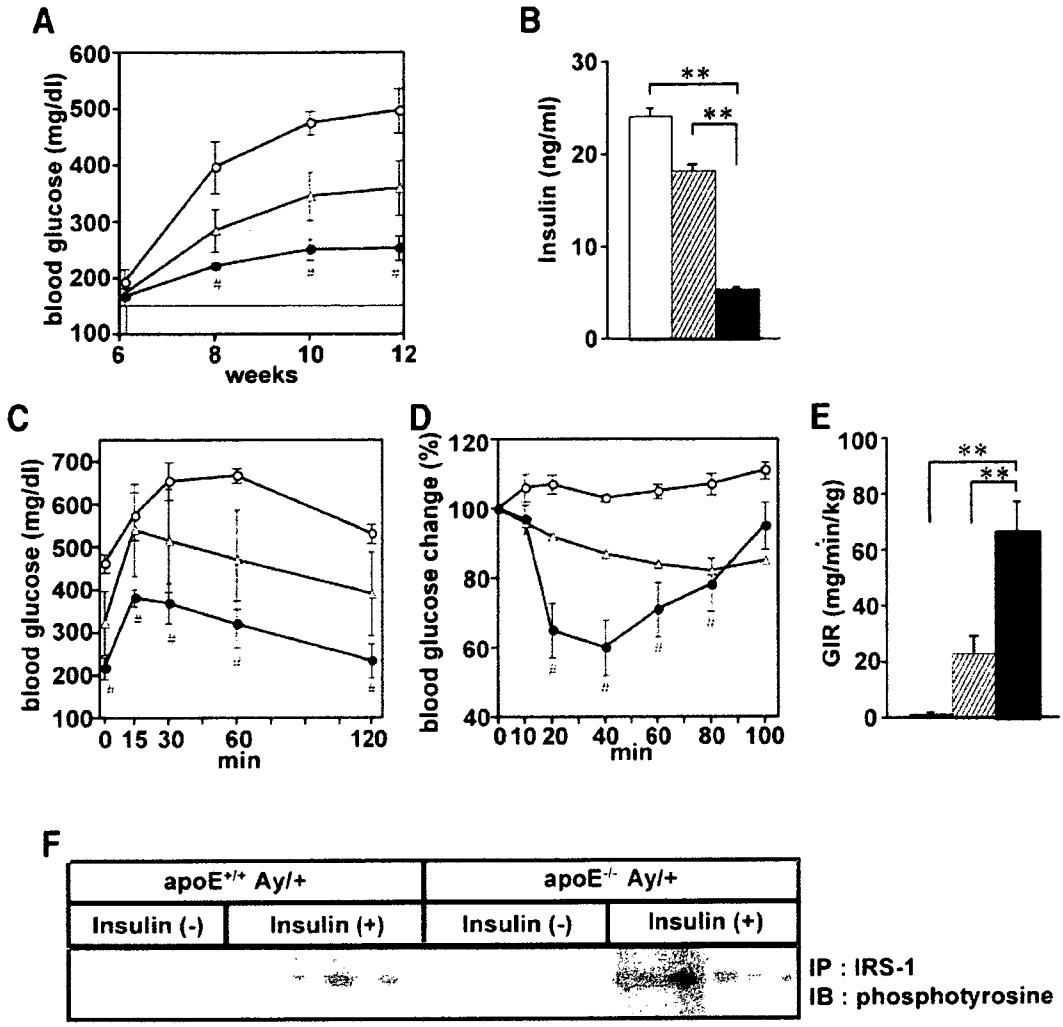

FIG. 2. ApoE deficiency improved glucose tolerance and insulin sensitivity in genetically obese mice. *A*: Fasting blood glucose levels were examined in apoE$^{+/+}$;Ay/+ (○), apoE$^{+/-}$;Ay/+ (△), and apoE$^{-/-}$;Ay/+ (●) mice biweekly from 6 to 12 weeks of age. *B*: Fasting plasma insulin levels of apoE$^{+/+}$;Ay/+ (□), apoE$^{+/-}$;Ay/+ (▨), and apoE$^{-/-}$;Ay/+ (■) mice were measured. *C* and *D*: Glucose tolerance (*C*) and insulin tolerance (*D*) tests were performed in apoE$^{+/+}$;Ay/+ (○), apoE$^{+/-}$;Ay/+ (△), and apoE$^{-/-}$;Ay/+ (●) mice. Data were expressed as percentages of blood glucose levels immediately before intraperitoneal insulin loading (n = 4–6 per group). *E*: Glucose infusion rates during hyperinsulinemic-euglycemic clamp studies were measured in apoE$^{+/+}$;Ay/+ (□), apoE$^{+/-}$;Ay/+ (▨), and apoE$^{-/-}$;Ay/+ (■) mice (n = 3 per group). *F*: Insulin-stimulated tyrosine phosphorylation of IRS-1 proteins in muscle. Mice that had been fasted for 16 h received an intravenous injection of 100 μl normal saline with or without insulin (10 units/kg body wt). Hindlimb muscles were removed 300 s later, and lysates were immunoprecipitated with anti–IRS-1 antibody. Immunoprecipitates were subjected to SDS-PAGE and immunoblotted with anti-phosphotyrosine antibody (4G10). Representative histological findings and immunoblots are presented. These metabolic studies in *B–F* were performed using 11-week-old mice. In *A–E*, data are presented graphically as means ± SE. *P < 0.05, **P < 0.01 by the unpaired t test and one-way ANOVA.

(Fig. 1*G*) and white (Fig. 1*H*) adipose tissues of apoE$^{-/-}$;Ay/+ mice were significantly smaller than those of apoE$^{+/+}$;Ay/+ mice. ApoE deficiency also decreased cell diameters in both brown (Fig. 1*I*) and white (Fig. 1*J*) adipose tissues. These findings suggest that apoE deficiency results in resistance to obesity via suppression of fat accumulation in the liver and fat tissues under obesity-inducing conditions.

ApoE deficiency induced greater glucose tolerance and insulin sensitivity in obese states. As described previously (15), lipid metabolism was markedly impaired with apoE deficiency (Supplemental Fig. 1*A* [online appendix]). Plasma cholesterol, triglyceride, and FFA levels were markedly higher in apoE$^{-/-}$;Ay/+ than in apoE$^{+/+}$;Ay/+ mice. HPLC analysis of plasma lipid profiles revealed that chylomicron, VLDL, and LDL fractions were markedly increased in apoE$^{-/-}$;Ay/+ compared with apoE$^{+/+}$;Ay/+ mice (Supplemental Fig. 1*B* [online appendix]).

Next, we examined the effects of apoE deficiency on glucose metabolism as well as insulin sensitivity in genetically obese Ay mice. From age 8 weeks onward, fasting blood glucose was markedly increased in apoE$^{+/+}$;Ay/+ mice on high-fat chow, but this glucose elevation was significantly inhibited by apoE deficiency (Fig. 2*A*). Fasting blood insulin levels at 11 weeks of age were lower, by 78%, in apoE$^{-/-}$;Ay/+ than in apoE$^{+/+}$;Ay/+ mice (Fig. 2*B*). Glucose (Fig. 2*C*) and insulin (Fig. 2*D*) tolerance tests documented that ApoE$^{-/-}$;Ay/+ mice were more glucose tolerant and insulin sensitive. We further examined insulin sensitivity using hyperinsulinemic-euglycemic clamp procedures. ApoE$^{+/+}$;Ay/+ mice fed high-fat chow exhibited severe insulin resistance, while in apoE$^{-/-}$;Ay/+ mice, glucose infusion rates were markedly higher, by 54-fold (Fig. 2*E*). Thus, despite hyperlipidemia, especially increased plasma FFA levels, apoE deficiency markedly

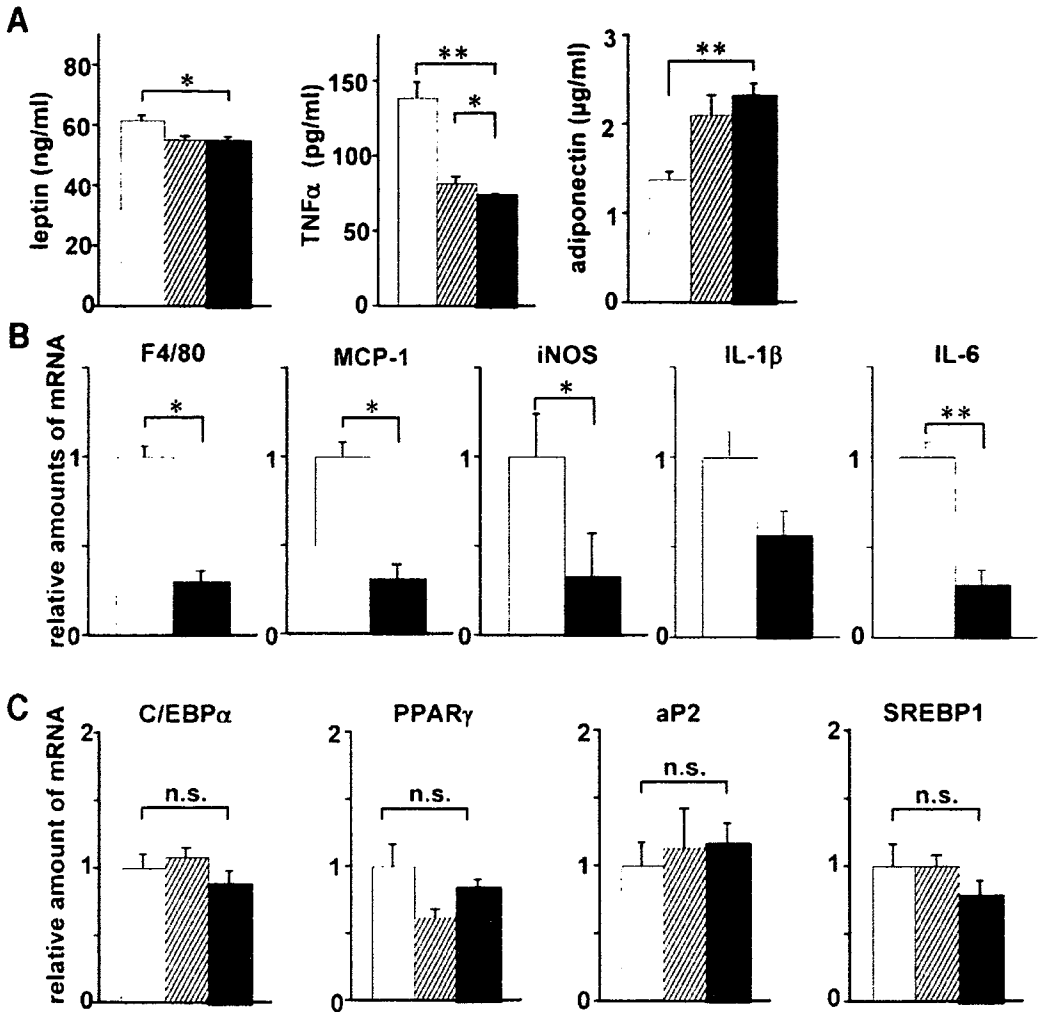

FIG. 3. ApoE deficiency affected plasma adipocytokine profiles and expressions of the mRNAs for inflammation- and differentiation-related proteins in adipose tissue. *A*: Plasma adipocytokines (*left*, leptin; *middle*, TNF-α; *right*, adiponectin) of high-fat chow–fed apoE$^{+/+}$;Ay/+ (□), apoE$^{+/-}$;Ay/+ (▨), and apoE$^{-/-}$;Ay/+ (■) mice were measured after a 10-h fast at 11 weeks of age. *B* and *C*: Relative amounts of mRNA in mesenteric white adipose tissue from apoE$^{+/+}$;Ay/+ (□) and apoE$^{-/-}$;Ay/+ (■) mice were determined by quantitative RT-PCR and corrected with 28S rRNA as the internal standard. Total RNA in white adipose tissue was isolated, after a 10-h fast, from 11-week-old mice. Levels of the mRNA levels for inflammation (*B*)- and differentiation (*C*)-related proteins in adipose tissue were assayed (n = 6 per group). Data are presented as means ± SE. *P < 0.05, **P < 0.01 by one-way ANOVA (*A*) and the unpaired t test (*B* and *C*).

improves glucose tolerance and insulin sensitivity. In addition, insulin-stimulated tyrosine phosphorylation of IRS-1 in muscle was enhanced in apoE$^{-/-}$;Ay/+ compared with apoE$^{+/+}$;Ay/+ mice (Fig. 2*F*). Thus, apoE deficiency apparently prevents surplus fat accumulation in adipose tissue and insulin resistance in muscle, resulting in better glucose tolerance.

Adipocytes are differentiated normally in apoE$^{-/-}$;Ay/+ mice in vivo. We next determined plasma adipocytokine profiles (Fig. 3*A*). In apoE$^{-/-}$;Ay/+ mice, plasma leptin levels were slightly decreased and TNF-α levels were markedly lower than those in apoE$^{+/+}$;Ay/+ mice, while plasma adiponectin levels were significantly higher. Thus, apoE deficiency improved obesity-induced alterations in adipocytokine profiles. In addition, quantitative RT-PCR revealed that expressions of F4/80, monocyte chemoattractant protein-1, inducible nitric oxide synthase, and interleukin-6 in mesenteric adipose tissue were significantly lower in apoE$^{-/-}$;Ay/+ than in apoE$^{+/+}$;Ay/+ mice (Fig. 3*B*), suggesting inhibition of inflammation and macrophage invasion into adipose tissue. Obesity is reportedly associated with macrophage infiltration of adipose tissue, which is likely to promote insulin resistance (27,28). Inhibition of macrophage invasion of adipose tissue may be involved in the higher insulin sensitivity and glucose tolerance observed in apoE$^{-/-}$;Ay/+ mice.

As described above, plasma adiponectin levels were increased in apoE$^{-/-}$;Ay/+ mice, suggesting normal adipocyte differentiation in vivo. Furthermore, mRNA expressions for adipocyte-related proteins, such as CCAAT/enhancer binding protein-α, peroxisome proliferator–activated receptor-γ, and aP2, were similar among adipose tissues from apoE$^{+/+}$;Ay/+, apoE$^{+/-}$;Ay/+, and apoE$^{-/-}$;Ay/+ mice (Fig. 3*C*). mRNA expressions levels of these three genes were also similar in adipose tissues from younger apoE$^{+/+}$;Ay/+ and apoE$^{-/-}$;Ay/+ mice, 4 weeks of age, when body weights were not significantly different (data not shown). In addition, apoE deficiency did not alter sterol regulatory element–binding protein 1 (SREBP1) expression (Fig. 3*C*). These findings indicate

that adipocytes are normally differentiated in apoE$^{-/-}$;Ay/+ mice in vivo.

Adenoviral apoE replenishment induced obesity and diabetes in genetically obese mice. To confirm that the metabolic phenotypes observed in apoE$^{-/-}$;Ay/+ mice were, in fact, mediated by apoE deficiency, we examined metabolic effects of adenovirus-mediated apoE expression in the livers of apoE$^{-/-}$;Ay/+ mice. Replenishment of apoE protein (human apoE3) resulted in markedly decreased plasma cholesterol, triglyceride, and FFA levels (Supplemental Fig. 2*A* [online appendix]), indicating functional expression of apoE. HPLC analyses of plasma lipid profiles revealed that adenoviral replenishment of apoE protein in apoE$^{-/-}$;Ay/+ mice markedly decreased the chylomicron and VLDL fractions (Supplemental Fig. 2*B* [online appendix]).

Increases in body weight for 7 days after adenoviral administration were significantly greater with the apoE adenovirus than with the LacZ control adenovirus (Fig. 4*A*). Liver weights tended to be increased (Fig. 4*B*), and those of brown adipose (Fig. 4*C*) and epididymal, mesenteric, and retroperitoneal white adipose (Fig. 4*D*) tissues were significantly increased with apoE adenoviral administration. Histological analyses revealed that apoE replenishment increased sizes of brown (Fig. 4*E* and *F*) and white (Fig. 4*G* and *H*) adipocytes. In addition, glucose tolerance tests revealed that apoE replenishment worsened glucose tolerance in apoE$^{-/-}$;Ay/+ mice (Fig. 4*I*). These findings show clearly that circulating apoE contributes to increased adiposity and the glucose intolerance associated with obesity. Furthermore, plasma leptin levels were significantly increased on day 7 after adenoviral administration. TNF-α and adiponectin levels tended to be increased and decreased, respectively (Fig. 4*J*), suggesting that circulating apoEs are involved in obesity-induced alterations in adipocytokine levels.

ApoE occurs in three major isoforms (apoE2, -E3, and -E4) in humans. ApoE3, the most common isoform, is considered to be the wild type. To compare the roles of the three human apoE isoforms in obesity and diabetes, recombinant adenoviruses encoding human apoE2 and -E4 as well as apoE3 were injected into apoE$^{-/-}$;Ay/+ mice. Administration of these apoE adenoviruses resulted in similar expression amounts of apoE proteins (data not shown), and similar increases in body weights (Supplemental Fig. 3*A* [online appendix]) and blood glucose levels (Supplemental Fig. 3*B* [online appendix]). These findings suggest that the three apoE isoforms contribute similarly to fat accumulation and glucose tolerance.

ApoE-less VLDL was uptaken into adipocytes, and the liver was impaired. Why does apoE deficiency inhibit obesity in genetically obese mice? We next examined the uptake of β-VLDL, with or without apoE, into fully differentiated 3T3-L1 adipocytes. β-VLDL obtained from apoE$^{-/-}$ mice was labeled with DiI, followed by incubation with or without recombinant human apoE3. As shown in Fig. 5*A*, uptake of apoE-deficient VLDL was markedly lower, by 85%, than that of apoE-positive (after incubation with human apoE3) VLDL. These findings suggest that impaired VLDL uptake into adipocytes contributes to decreased adiposity in apoE$^{-/-}$;Ay/+ mice. Thus, VLDL uptake into adipocytes is likely to play a role in excess fat deposition and, thereby, in the development of diabetes associated with obesity.

ApoE deficiency reportedly reduces hepatic VLDL secretion, resulting in fatty liver findings (11). In our model as well, hepatic triglyceride secretion was inhibited in apoE$^{-/-}$;Ay/+ mice compared with apoE$^{+/+}$;Ay/+ mice, by 48% (Fig. 5*B*). However, interestingly, apoE$^{-/-}$;Ay/+ mice displayed less fat accumulation in the liver than apoE$^{+/+}$;Ay/+ mice (Fig. 1*D–F*). To elucidate the underlying mechanism, we examined β-VLDL uptake into the liver. Fluorescence-labeled β-VLDL, with or without apoE, was intravenously injected into wild-type C57BL/6 mice. Fluorescence values in the liver were then measured. Uptake of apoE-deficient β-VLDL was markedly lower, by 49%, than that of apoE-positive VLDL (Fig. 5*C*). Thus, despite decreased secretion, decreased β-VLDL uptake with apoE deficiency may contribute to prevention of hepatic steatosis. Therefore, apoE is likely to be involved in excess fat uptake into hepatocytes as well as adipocytes. Taken together with the findings that adenoviral apoE replenishment decreased the VLDL fraction (Supplemental Fig. 2*B* [online appendix]), our results indicate that apoE-dependent VLDL transport into tissues, including the liver and adipose tissue, is involved in the development of obesity, resulting in glucose intolerance and insulin resistance.

ApoE deficiency decreased food intake and increased energy expenditure in genetically obese mice. Next, to elucidate the systemic mechanism underlying the obesity prevention associated with apoE deficiency, we first measured food intakes in apoE$^{+/+}$;Ay/+ and apoE$^{-/-}$;Ay/+ mice. Interestingly, apoE deficiency in Ay mice significantly suppressed food intake (Fig. 5*D*). Then, to eliminate the secondary effects of reduced food intake in apoE$^{-/-}$;Ay/+ mice, ApoE$^{+/+}$;Ay/+ mice were allotted the same amounts of food consumption as apoE$^{-/-}$;Ay/+ mice, followed by weight measurement and glucose tolerance testing. Pair-feeding blunted the body weight increments in apoE$^{+/+}$;Ay/+ mice, while the weights of pair-fed apoE$^{+/+}$;Ay/+ mice were significantly greater than those of apoE$^{-/-}$;Ay/+ mice (Fig. 5*E*). ApoE$^{-/-}$;Ay/+ mice exhibited better glucose tolerance than pair-fed apoE$^{+/+}$;Ay/+ mice (Fig. 5*F*). Thus, the inhibition of obesity and glucose intolerance by apoE deficiency is not attributable solely to decreased food intake.

Next, we measured basal metabolic rates. As shown in Fig. 5*G*, resting oxygen consumption in both the light and the dark phase at 5 weeks of age was significantly greater in apoE$^{-/-}$;Ay/+ than in apoE$^{+/+}$;Ay/+ mice. Taken together with the pair-feeding experiment results, these findings show that decreased food intake and increased energy expenditure both contribute to the prevention of obesity and insulin resistance with apoE deficiency and that apoE is involved in regulation of energy metabolism.

DISCUSSION

To examine the effects of apoE deficiency on insulin resistance associated with obesity, apoE$^{-/-}$ mice were interbred with KK-Ay mice. ApoE$^{-/-}$;Ay/+ mice showed resistance to the development of obesity and glucose intolerance. Insulin sensitivity was markedly greater in apoE$^{-/-}$;Ay/+ than in apoE$^{+/+}$;Ay/+ mice. Recently, several attempts to induce obesity in apoE$^{-/-}$ mice have been reported, but the results have been somewhat controversial (12–14). In the present study, in addition to inhibition of adiposity and insulin resistance with apoE deficiency, adenoviral apoE replenishment reversed inhibition of obesity and glucose intolerance. These findings directly demonstrate apoE involvement in the development of obesity and obesity-related disorders of glucose metabolism and insulin sensitivity. Chiba et al. (14) previously reported

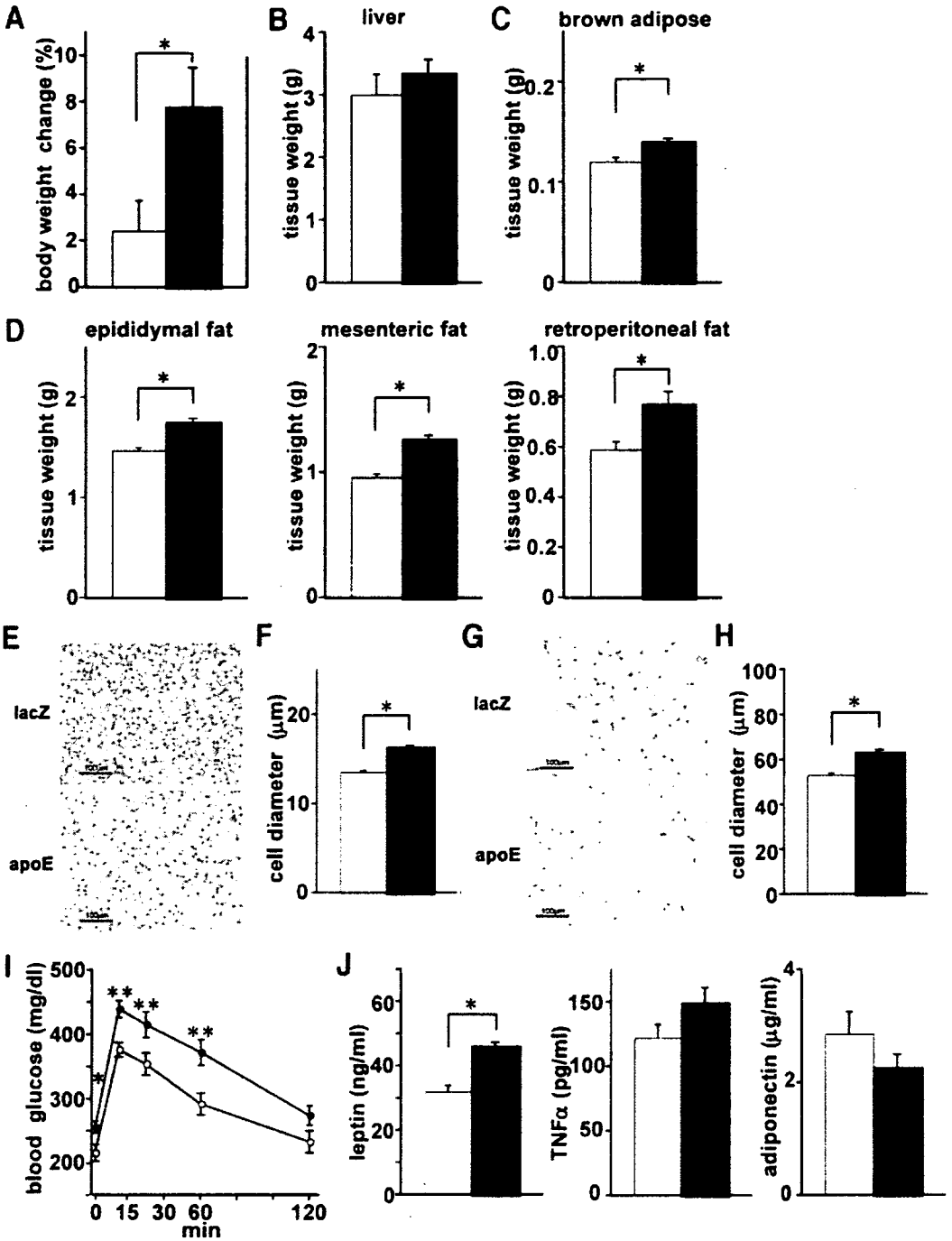

FIG. 4. Adenoviral apoE replenishment induced obesity and diabetes in genetically obese mice. ApoE$^{-/-}$;Ay/+ mice were intravenously administered LacZ (□ or ○) or apoE (■ or ●) adenovirus at 10 weeks of age after 4 weeks of high-fat loading. *A*: Body weight changes for 7 days after adenoviral administration were examined. *B–D*: Weights of the liver (*B*) and brown adipose (*C*) as well as white adipose (*D*: *left*, epididymal fat; *middle*, mesenteric fat; *right*, retroperitoneal fat) tissues were determined on day 7 after adenoviral injection (n = 6 per group). *E–H*: Histological findings of brown adipose (*E* and *F*) and mesenteric white adipose (*G* and *H*) tissues. Representative hematoxylin-eosin stained tissue samples are presented (*E* and *G*). Cell diameters were measured in these tissues (*F* and *H*). *I*: Glucose tolerance tests were performed on day 7 after adenoviral injection (n = 5–8 per group). *J*: Plasma adipocytokine levels (*left*, leptin; *middle*, TNF-α; *right*, adiponectin) were assayed on day 7 after adenoviral injection (n = 5–8 per group). Data are presented as means ± SE. *P < 0.05, **P < 0.01 by the unpaired t test.

that *ob/ob*;apoE$^{-/-}$ mice are also resistant to obesity. They attributed decreased adiposity in *ob/ob*;apoE$^{-/-}$ mice to impaired adipocyte differentiation based on in vitro findings that expression levels of aP2 and peroxisome proliferator–activated receptor-γ were markedly lower when bone marrow stromal cells and 3T3-L1 cells were cultured with apoE-less VLDL. However, in the present study, adipocytes in apoE$^{-/-}$;Ay/+ mice expressed these adipocyte-related proteins normally in vivo. Furthermore, apoE$^{-/-}$;Ay/+ mice showed better insulin sensitivity and less hepatic lipid accumulation, accompanied by improved adipocytokine profiles, than apoE$^{+/+}$;Ay/+ mice. Thus,

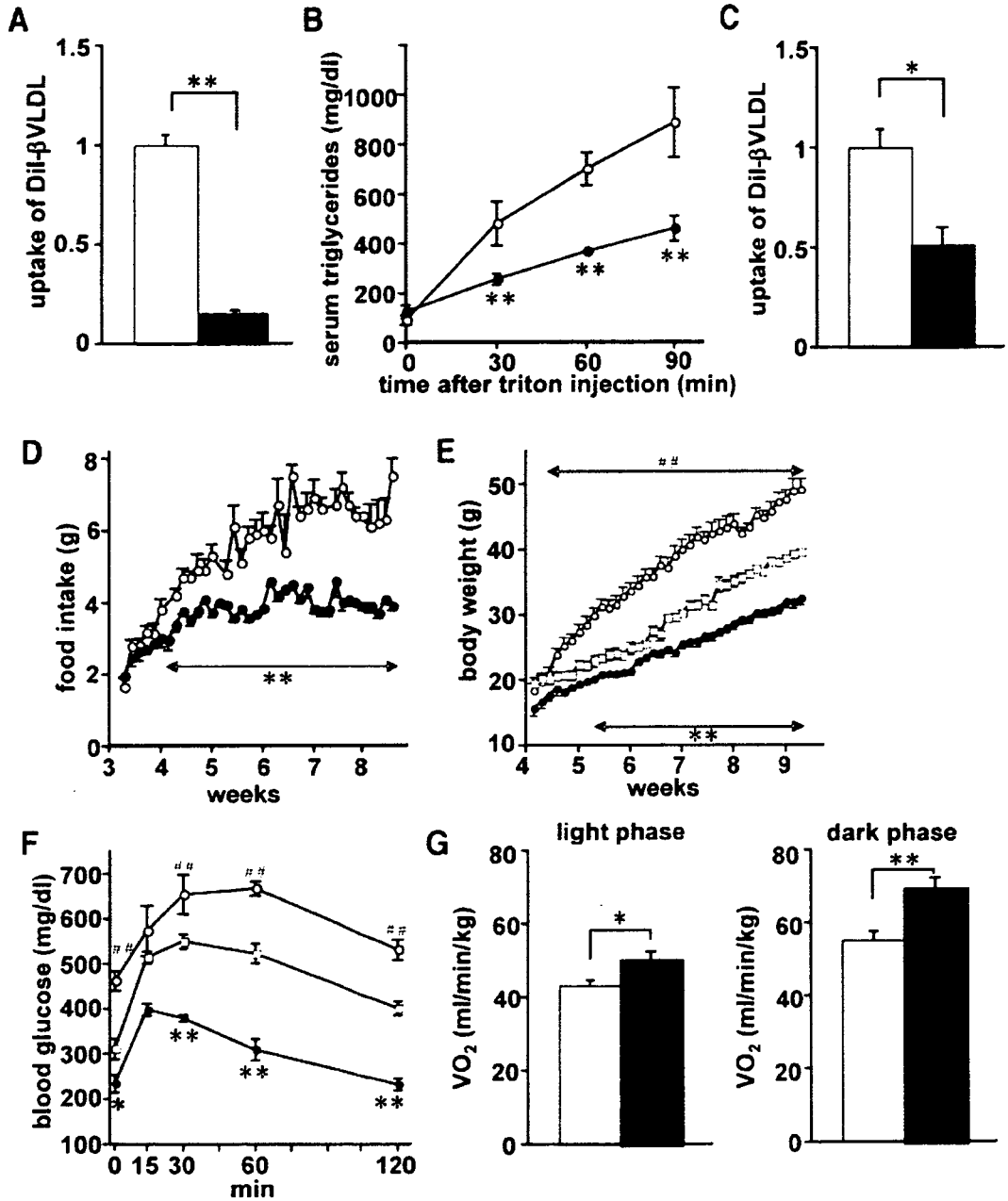

FIG. 5. ApoE deficiency inhibited β-VLDL uptake into adipocytes and the liver, decreased food intake, and increased energy expenditure. *A*: Uptakes of fluorescence-labeled β-VLDL, with (□) or without (■) apoE, into cultured adipocytes were measured. β-VLDL was isolated from apoE$^{-/-}$ mouse sera, followed by labeling with DiI and pretreatment with or without human recombinant apoE3. Fully differentiated 3T3-L1 adipocytes were incubated with apoE-positive or apoE-less β-VLDL for 8 h, followed by measurement of fluorescence uptake into adipocytes. Data are presented as the relative amounts of β-VLDL uptake compared with apoE-positive β-VLDL uptake (n = 6 per group). *B*: Triglyceride secretion rates from the liver after administration of Triton WR-1339 were measured in 11-week-old apoE$^{+/+}$;Ay/+ (○) and apoE$^{-/-}$;Ay/+ (●) mice fed a high-fat diet for 5 weeks. *C*: Hepatic uptake of β-VLDL with or without apoE. Fluorescence-labeled β-VLDL with or without apoE was intravenously injected into 11-week-old apoE$^{+/+}$;Ay/+ mice fed a high-fat diet for 5 weeks, followed by measurement of fluorescence levels in the liver 30 min after injection. Data are presented as the relative amounts of β-VLDL uptake compared with apoE-positive β-VLDL uptake (n = 4 per group). *D*: Daily food intake amounts from weaning through 8 weeks of age are presented. *E* and *F*: ApoE$^{+/+}$;Ay/+ mice were allotted into two groups at 4 weeks of age, and one group of apoE$^{+/+}$;Ay/+mice was given their daily food allotments based on the previous days' consumption by apoE$^{-/-}$;Ay/+ littermate mice. Body weights (*E*) were determined and glucose tolerance tests (*F*) were performed in apoE$^{+/+}$;Ay/+ mice (○), pair-fed apoE$^{+/+}$;Ay/+ mice (□), and apoE$^{-/-}$;Ay/+ mice (●) (n = 6–8 per group). *G*: Resting oxygen consumption in the light and dark phases was measured at 5 weeks of age with open-circuit indirect calorimetry. n = 4 per group. Data are presented as means ± SE. *P < 0.05, **P < 0.01 by the unpaired t test. In *E* and *F* ##P < 0.01 for pair-feeding apoE$^{+/+}$;Ay/+ mice versus apoE$^{+/+}$;Ay/+ mice; *P < 0.05, **P < 0.01 for pair-feeding apoE$^{+/+}$;Ay/+ mice versus apoE$^{-/-}$;Ay/+ mice, by one-way ANOVA.

decreased adiposity and improved insulin sensitivity in apoE$^{-/-}$;Ay/+ mice can be explained by factors other than adipocyte differentiation.

While body weight and adiposity were similar in young apoE$^{-/-}$ and apoE$^{+/+}$ mice, apoE deficiency ameliorated obesity and insulin resistance under obesity-inducing con-

ditions, such as aging, genetic susceptibility, and dietary loading, suggesting that apoE is involved in obesity development, i.e., excess fat accumulation, while being less involved in basal fat accumulation. Lack of apoE in β-VLDL markedly impaired β-VLDL transport into adipocytes. ApoE is an important component of VLDL. There are several receptors, including VLDL receptor (VLDLR) and LDL receptor–related protein, which recognize VLDL in an apoE-dependent manner (22). Among them, VLDLRs reportedly have similar affinities for apoE2, -E3, and -E4 isoforms (29). In addition, VLDLR-deficient mice reportedly exhibit obesity resistance with high-fat chow loading (30). Taken together with our findings that replenishment of apoE2, -E3, and -E4 isoforms contributes similarly to fat accumulation and glucose tolerance in apoE$^{-/-}$;Ay/+ mice, the apoE-VLDLR interaction plays an important role in the development of obesity. Furthermore, it is well known that high levels of plasma VLDL are associated with obesity and type 2 diabetes (31). Thus, receptor-mediated VLDL transport into adipocytes in an apoE-dependent manner is involved mainly in excess lipid uptake into adipocytes. Lipid uptake, required for adipocyte differentiation and metabolic activities, might be mediated mainly by apoE-independent lipid transport pathways or de novo lipid synthesis in adipocytes.

In addition, transport of apoE-deficient β-VLDL into the liver was markedly impaired compared with that of apoE-positive β-VLDL. Despite decreased triglyceride secretion, apoE deficiency decreased hepatic fat accumulation in Ay, but not in wild-type, mice (11). Hepatic expressions of SREBP1c and fatty acid synthase were similar in apoE$^{-/-}$;Ay/+ and apoE$^{+/+}$;Ay/+ mice (data not shown), suggesting no apparent decrease in hepatic fatty acid synthesis in apoE$^{-/-}$;Ay/+ mice. These findings suggest that apoE-dependent uptake of β-VLDL into hepatocytes is involved in the development of hepatic steatosis in Ay mice. The machinery that transports β-VLDL into the liver, including the receptor(s) playing a major role, is a potential target for elucidating the mechanism underlying hepatic steatosis.

Intriguingly, in apoE$^{-/-}$;Ay/+ mice, food intake was decreased and energy expenditure enhanced compared with apoE$^{+/+}$;Ay/+ mice. Pair-feeding experiments revealed that both these phenomena result in obesity resistance in apoE$^{-/-}$;Ay/+ mice. There appear to be several possible explanations for these alterations in energy metabolism. First, hyperlipidemia induced by apoE deficiency might contribute to decreased food intake and increased energy expenditure. However, LDLR$^{-/-}$ mice, which also exhibit hyperlipidemia, reportedly become more obese and diabetic in response to high-fat and high-carbonate diets than wild-type mice (13). In addition, food intake was similar in LDLR$^{-/-}$ mice and LDLR$^{+/+}$ mice (13). Therefore, although hyperlipidemia is more severe in apoE$^{-/-}$ than in LDLR$^{-/-}$ mice, involvement of hyperlipidemia in food intake regulation might be unlikely in our model. Second, we speculate that leptin sensitization is involved in decreased food intake and increased energy expenditure. Obesity is well known to be associated with poor responses to leptin despite hyperleptinemia, a state defined as leptin resistance (32). Lower plasma leptin levels with lower body weight in apoE$^{-/-}$;Ay/+ mice compared with apoE$^{+/+}$;Ay/+ mice suggests greater leptin sentivity in the former. Therefore, decreased food intake and increased energy expenditure in apoE$^{-/-}$;Ay/+ mice might be explained by leptin sensitization. We have recently reported that alterations in metabolism in adipose tissue affect food intake amounts (19). However, *ob/ob*;apoE$^{-/-}$ mice are also reportedly resistant to obesity (14). Since *ob/ob* mice are leptin deficient, the obesity resistance in *ob/ob*;apoE$^{-/-}$ mice is not mediated by leptin signaling, e.g., leptin sensitization, although food intake and energy expenditure were not measured in the earlier study (14). Thus, mechanisms other than leptin sensitization might be involved in decreased food intake and increased energy expenditure in apoE$^{-/-}$;Ay/+ mice. Third, direct effects of apoE on neurons are also possible. ApoE, produced by glial cells, is a major apolipoprotein in the brain and mediates the transport of cholesterol and phospholipids, and its receptors are abundantly expressed on neurons (33). Furthermore, numerous studies have shown that apoE plays multiple roles in the nervous system. In the central and peripheral nervous systems, apoE promotes neurite outgrowth and regeneration (34). ApoE protects neurons from oxidative injury (35) and modulates amyloid-β deposition (36), interactions with Alzheimer amyloid precursor protein (37), and transmission of signals to neurons (38). In this context, modulation of neurons by apoE might be involved in energy metabolism. ApoE is reportedly expressed in tissues other than the liver, including the brain (33) and adipose tissue (39). ApoE deficiency in these tissues may affect the metabolic phenotypes of apoE$^{-/-}$;Ay/+ mice observed herein. Intensive research, including tissue-specific disruption of apoE or its receptor, is required to examine this hypothesis.

ApoE is involved in surplus fat accumulation and energy metabolism, including regulation of food intake and energy expenditure. Thus, excess fat accumulation via an apoE-dependent pathway might play a role in development of the metabolic syndrome. In addition to dissipation of surplus energy (4), apoE-dependent excess lipid transport is a potentially novel therapeutic target for the metabolic syndrome.

ACKNOWLEDGMENTS

This work was supported by a Grant-in-Aid for Scientific Research (B2, 15390282) to H.K.; a Grant-in-Aid for Scientific Research (17790599) to Y.I. from the Ministry of Education, Science, Sports and Culture of Japan; and a Grant-in-Aid for Scientific Research (H16-genome-003) to Y.O. from the Ministry of Health, Labor and Welfare of Japan. This work was also supported by the 21st Century COE Programs "CRESCENDO" to H.K. and "the Center for Innovative Therapeutic Development for Common Diseases" to Y.O. from the Ministry of Education Science, Sports and Culture.

We thank I. Sato, J. Fushimi, K. Kawamura, and M. Hoshi for technical support.

REFERENCES

1. Eckel RH, Grundy SM, Zimmet PZ: The metabolic syndrome. *Lancet* 365:1415–1428, 2005
2. Fruhbeck G, Gomez-Ambrosi J: Control of body weight: a physiologic and transgenic perspective. *Diabetologia* 46:143–172, 2003
3. Friedman JM: A war on obesity, not the obese. *Science* 299:856–858, 2003
4. Ishigaki Y, Katagiri H, Yamada T, Ogihara T, Imai J, Uno K, Hasegawa Y, Gao J, Ishihara H, Shimosegawa T, Sakoda H, Asano T, Oka Y: Dissipating excess energy stored in the liver is a potential treatment strategy for diabetes associated with obesity. *Diabetes* 54:322–332, 2005
5. Moitra J, Mason MM, Olive M, Krylov D, Gavrilova O, Marcus-Samuels B, Feigenbaum L, Lee E, Aoyama T, Eckhaus M, Reitman ML, Vinson C: Life without white fat: a transgenic mouse. *Genes Dev* 12:3168–3181, 1998
6. Shimomura I, Hammer RE, Richardson JA, Ikemoto S, Bashmakov Y,

Goldstein JL, Brown MS: Insulin resistance and diabetes mellitus in transgenic mice expressing nuclear SREBP-1c in adipose tissue: model for congenital generalized lipodystrophy. *Genes Dev* 12:3182–3194, 1998
7. Oral EA, Simha V, Ruiz E, Andewelt A, Premkumar A, Snell P, Wagner AJ, DePaoli AM, Reitman ML, Taylor SI, Gorden P, Garg A: Leptin-replacement therapy for lipodystrophy. *N Engl J Med* 346:570–578, 2002
8. Hussain MM, Maxfield FR, Mas-Oliva J, Tabas I, Ji ZS, Innerarity TL, Mahley RW: Clearance of chylomicron remnants by the low density lipoprotein receptor-related protein/alpha 2-macroglobulin receptor. *J Biol Chem* 266:13936–13940, 1991
9. Chappell DA, Medh JD: Receptor-mediated mechanisms of lipoprotein remnant catabolism. *Prog Lipid Res* 37:393–422, 1998
10. Cooper AD: Hepatic uptake of chylomicron remnants. *J Lipid Res* 38:2173–2192, 1997
11. Kuipers F, Jong MC, Lin Y, Eck M, Havinga R, Bloks V, Verkade HJ, Hofker MH, Moshage H, Berkel TJ, Vonk RJ, Havekes LM: Impaired secretion of very low density lipoprotein-triglycerides by apolipoprotein E-deficient mouse hepatocytes. *J Clin Invest* 100:2915–2922, 1997
12. Lyngdorf LG, Gregersen S, Daugherty A, Falk E: Paradoxical reduction of atherosclerosis in apoE-deficient mice with obesity-related type 2 diabetes. *Cardiovasc Res* 59:854–862, 2003
13. Schreyer SA, Vick C, Lystig TC, Mystkowski P, LeBoeuf RC: LDL receptor but not apolipoprotein E deficiency increases diet-induced obesity and diabetes in mice. *Am J Physiol Endocrinol Metab* 282:E207–E214, 2002
14. Chiba T, Nakazawa T, Yui K, Kaneko E, Shimokado K: VLDL induces adipocyte differentiation in ApoE-dependent manner. *Arterioscler Thromb Vasc Biol* 23:1423–1429, 2003
15. Zhang SH, Reddick RL, Piedrahita JA, Maeda N: Spontaneous hypercholesterolemia and arterial lesions in mice lacking apolipoprotein E. *Science* 258:468–471, 1992
16. Ishigaki Y, Oikawa S, Suzuki T, Usui S, Magoori K, Kim DH, Suzuki H, Sasaki J, Sasano H, Okazaki M, Toyota T, Saito T, Yamamoto TT: Virus-mediated transduction of apolipoprotein E (ApoE)-sendai develops lipoprotein glomerulopathy in ApoE-deficient mice. *J Biol Chem* 275: 31269–31273, 2000
17. Anai M, Funaki M, Ogihara T, Terasaki J, Inukai K, Katagiri H, Fukushima Y, Yazaki Y, Kikuchi M, Oka Y, Asano T: Altered expression levels and impaired steps in the pathway to phosphatidylinositol 3-kinase activation via insulin receptor substrates 1 and 2 in Zucker fatty rats. *Diabetes* 47:13–23, 1998
18. Usui S, Hara Y, Hosaki S, Okazaki M: A new on-line dual enzymatic method for simultaneous quantification of cholesterol and triglycerides in lipoproteins by HPLC. *J Lipid Res* 43:805–814, 2002
19. Yamada T, Katagiri H, Ishigaki Y, Ogihara T, Imai J, Uno K, Hasegawa Y, Gao J, Ishihara H, Niijima A, Mano H, Aburatani H, Asano T, Oka Y: Signals from intra-abdominal fat modulate insulin and leptin sensitivity through different mechanisms: neuronal involvement in food-intake regulation. *Cell Metab* 3:223–229, 2006
20. Uno K, Katagiri H, Yamada T, Ishigaki Y, Ogihara T, Imai J, Hasegawa Y, Gao J, Kaneko K, Iwasaki H, Ishihara H, Sasano H, Inukai K, Mizuguchi H, Asano T, Shiota M, Nakazato M, Oka Y: Neuronal pathway from the liver modulates energy expenditure and systemic insulin sensitivity. *Science* 312:1656–1659, 2006
21. Min J, Okada S, Kanzaki M, Elmendorf JS, Coker KJ, Ceresa BP, Syu LJ, Noda Y, Saltiel AR, Pessin JE: Synip: a novel insulin-regulated syntaxin 4-binding protein mediating GLUT4 translocation in adipocytes. *Mol Cell* 3:751–760, 1999
22. Takahashi S, Kawarabayasi Y, Nakai T, Sakai J, Yamamoto T: Rabbit very low density lipoprotein receptor: a low density lipoprotein receptor-like protein with distinct ligand specificity. *Proc Natl Acad Sci U S A* 89:9252–9256, 1992
23. Descamps O, Bilheimer D, Herz J: Insulin stimulates receptor-mediated uptake of apoE-enriched lipoproteins and activated alpha 2-macroglobulin in adipocytes. *J Biol Chem* 268:974–981, 1993
24. Wilsie LC, Chanchani S, Navaratna D, Orlando RA: Cell surface heparan sulfate proteoglycans contribute to intracellular lipid accumulation in adipocytes. *Lipids Health Dis* 4:2, 2005
25. Siri P, Candela N, Zhang YL, Ko C, Eusufzai S, Ginsberg HN, Huang LS: Post-transcriptional stimulation of the assembly and secretion of triglyceride-rich apolipoprotein B lipoproteins in a mouse with selective deficiency of brown adipose tissue, obesity, and insulin resistance. *J Biol Chem* 276:46064–46072, 2001
26. Fujino T, Asaba H, Kang MJ, Ikeda Y, Sone H, Takada S, Kim DH, Ioka RX, Ono M, Tomoyori H, Okubo M, Murase T, Kamataki A, Yamamoto J, Magoori K, Takahashi S, Miyamoto Y, Oishi H, Nose M, Okazaki M, Usui S, Imaizumi K, Yanagisawa M, Sakai J, Yamamoto TT: Low-density lipoprotein receptor-related protein 5 (LRP5) is essential for normal cholesterol metabolism and glucose-induced insulin secretion. *Proc Natl Acad Sci U S A* 100:229–234, 2003
27. Xu H, Barnes GT, Yang Q, Tan G, Yang D, Chou CJ, Sole J, Nichols A, Ross JS, Tartaglia LA, Chen H: Chronic inflammation in fat plays a crucial role in the development of obesity-related insulin resistance. *J Clin Invest* 112:1821–1830, 2003
28. Weisberg SP, McCann D, Desai M, Rosenbaum M, Leibel RL, Ferrante AW Jr: Obesity is associated with macrophage accumulation in adipose tissue. *J Clin Invest* 112:1796–1808, 2003
29. Takahashi S, Oida K, Ookubo M, Suzuki J, Kohno M, Murase T, Yamamoto T, Nakai T: Very low density lipoprotein receptor binds apolipoprotein E2/2 as well as apolipoprotein E3/3. *FEBS Lett* 386:197–200, 1996
30. Goudriaan JR, Tacken PJ, Dahlmans VE, Gijbels MJ, van Dijk KW, Havekes LM, Jong MC: Protection from obesity in mice lacking the VLDL receptor. *Arterioscler Thromb Vasc Biol* 21:1488–1493, 2001
31. Reaven GM: Banting lecture 1988: Role of insulin resistance in human disease. *Diabetes* 37:1595–1607, 1988
32. Considine RV, Sinha MK, Heiman ML, Kriauciunas A, Stephens TW, Nyce MR, Ohannesian JP, Marco CC, McKee LJ, Bauer TL, et al.: Serum immunoreactive-leptin concentrations in normal-weight and obese humans. *N Engl J Med* 334:292–295, 1996
33. Mahley RW, Nathan BP, Pitas RE: Apolipoprotein E: structure, function, and possible roles in Alzheimer's disease. *Ann N Y Acad Sci* 777:139–145, 1996
34. Masliah E, Mallory M, Ge N, Alford M, Veinbergs I, Roses AD: Neurodegeneration in the central nervous system of apoE-deficient mice. *Exp Neurol* 136:107–122, 1995
35. Chen Y, Lomnitski L, Michaelson DM, Shohami E: Motor and cognitive deficits in apolipoprotein E-deficient mice after closed head injury. *Neuroscience* 80:1255–1262, 1997
36. Bales KR, Verina T, Dodel RC, Du Y, Altstiel L, Bender M, Hyslop P, Johnstone EM, Little SP, Cummins DJ, Piccardo P, Ghetti B, Paul SM: Lack of apolipoprotein E dramatically reduces amyloid beta-peptide deposition. *Nat Genet* 17:263–264, 1997
37. Barger SW, Harmon AD: Microglial activation by Alzheimer amyloid precursor protein and modulation by apolipoprotein E. *Nature* 388:878–881, 1997
38. Trommsdorff M, Gotthardt M, Hiesberger T, Shelton J, Stockinger W, Nimpf J, Hammer RE, Richardson JA, Herz J: Reeler/disabled-like disruption of neuronal migration in knockout mice lacking the VLDL receptor and ApoE receptor 2. *Cell* 97:689–701, 1999
39. Zechner R, Moser R, Newman TC, Fried SK, Breslow JL: Apolipoprotein E gene expression in mouse 3T3–L1 adipocytes and human adipose tissue and its regulation by differentiation and lipid content. *J Biol Chem* 266:10583–10588, 1991